Laboratoř růstových regulátorů

Miroslav Strnad

Fotosyntéza-světelné reakce [kap 7]

- Univerzita Palackého & Ústav experimentální botaniky AV CR

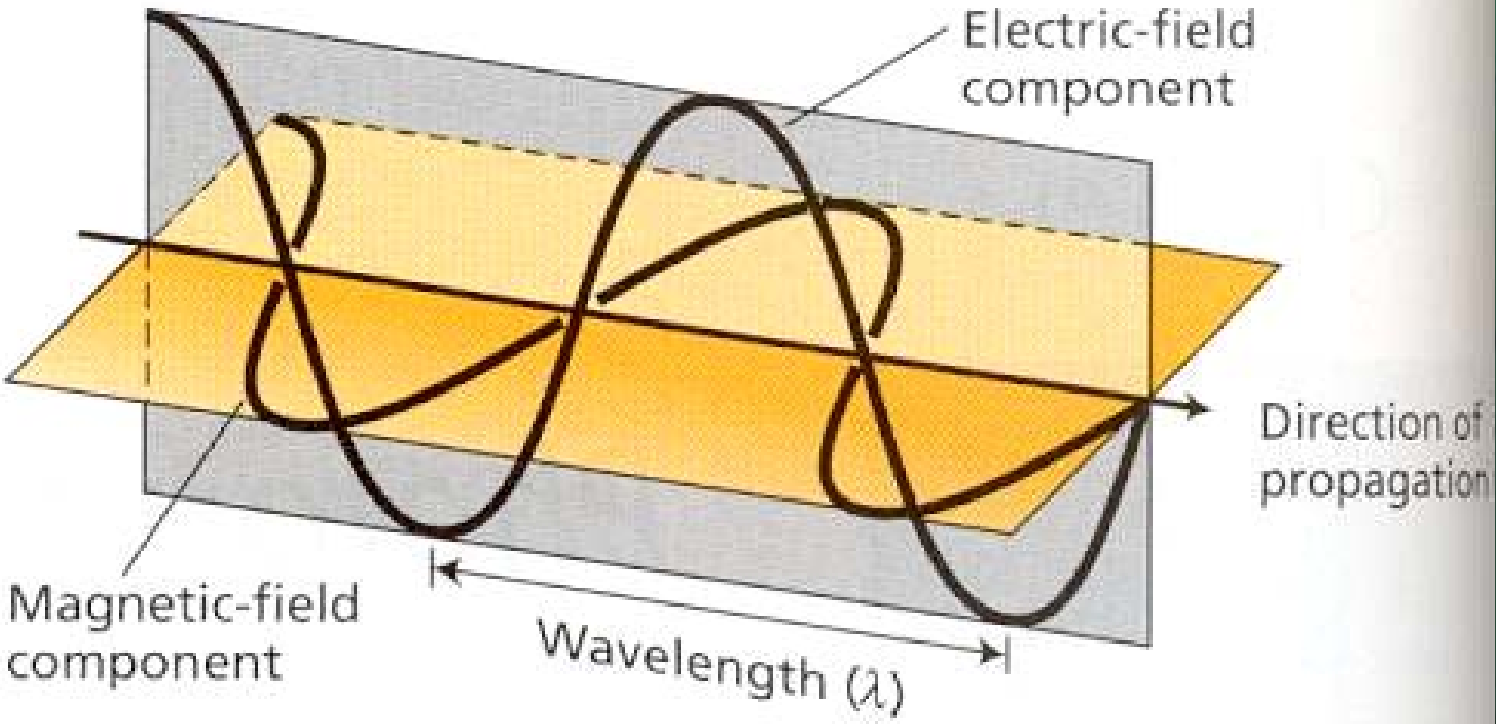

FIGURE 7.1 Light is a transverse electromagnetic wave, consisting of oscillating electric and magnetic fields that are perpendicular to each other and to the direction of propagation of the light. Light moves at a speed of 3×10^8 m s^{-1}. The wavelength (λ) is the distance between successive crests of the wave.

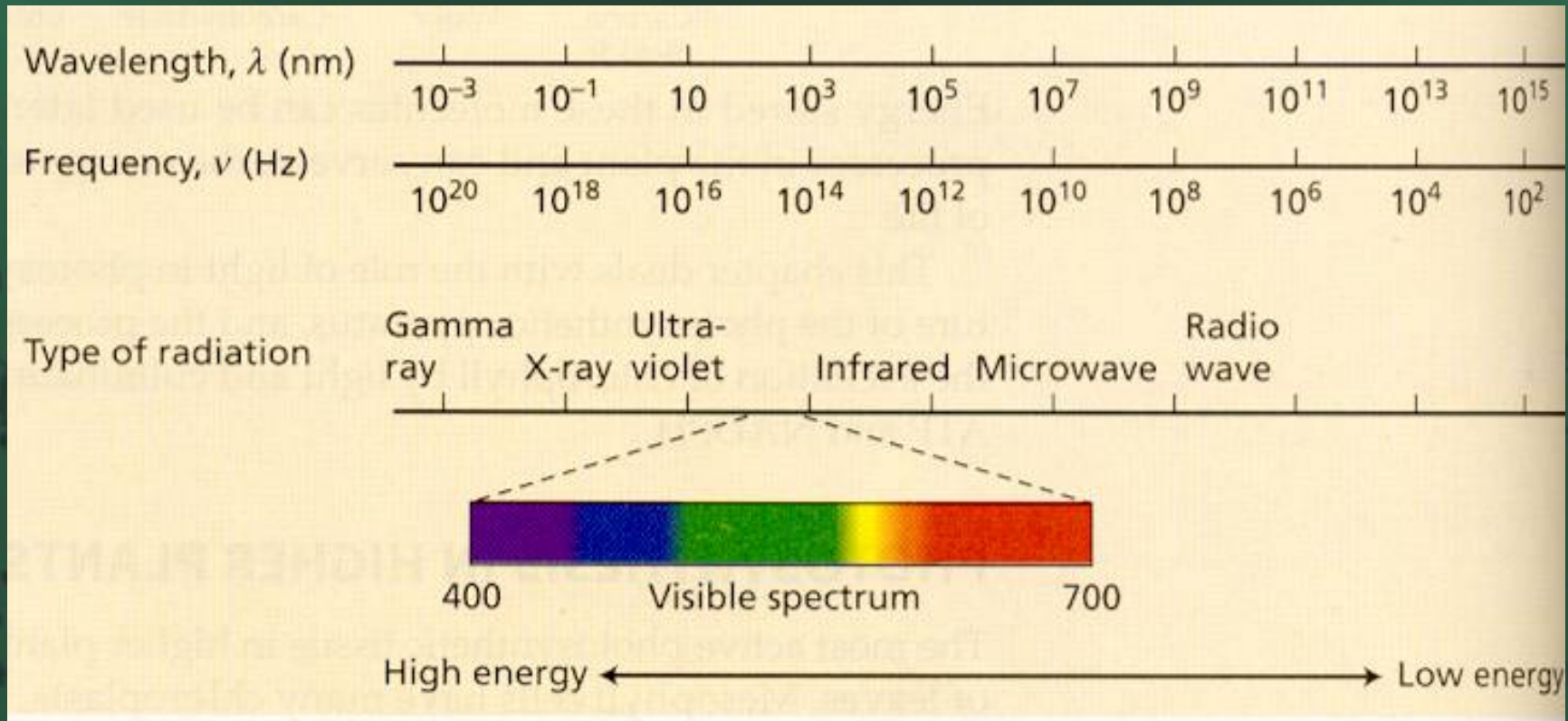

FIGURE 7.2 Electromagnetic spectrum. Wavelength (λ) and frequency (ν) are inversely related. Our eyes are sensitive to only a narrow range of wavelengths of radiation, the visible region, which extends from about 400 nm (violet) to about 700 nm (red). Short-wavelength (high-frequency) light has a high energy content; long-wavelength (low-frequency) light has a low energy content.

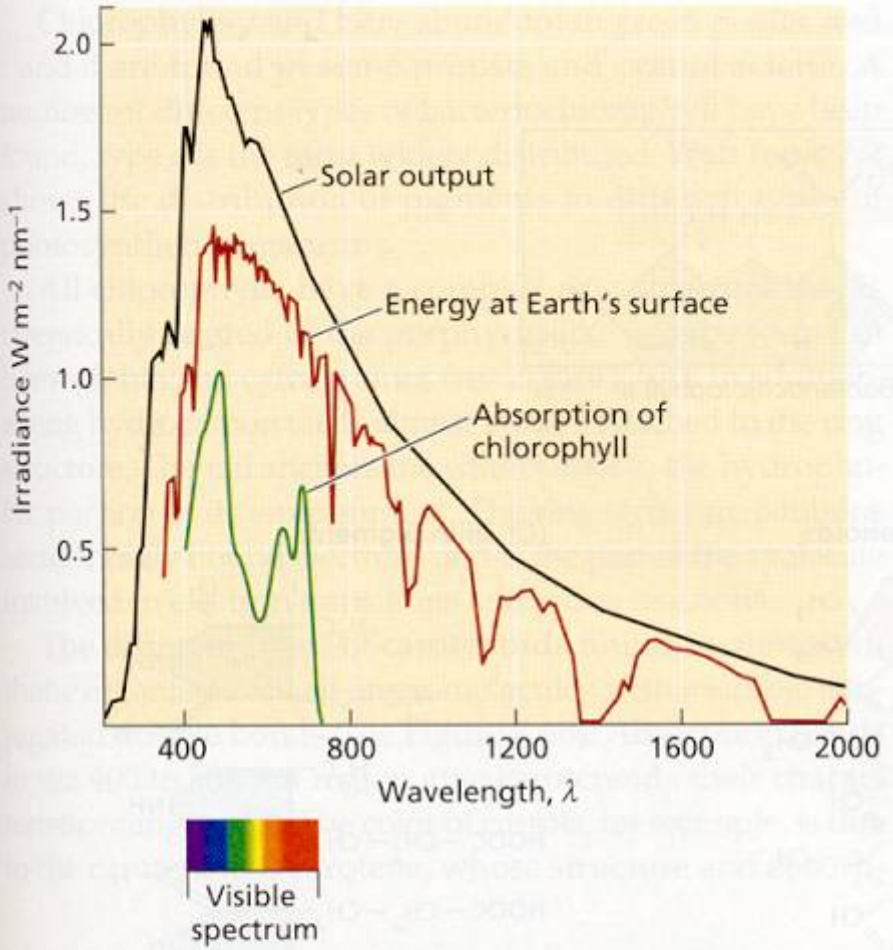

FIGURE 7.3 The solar spectrum and its relation to the absorption spectrum of chlorophyll. Curve A is the energy output of the sun as a function of wavelength. Curve B is the energy that strikes the surface of Earth. The sharp valleys in the infrared region beyond 700 nm represent the absorption of solar energy by molecules in the atmosphere, chiefly water vapor. Curve C is the absorption spectrum of chlorophyll, which absorbs strongly in the blue (about 430 nm) and the red (about 660 nm) portions of the spectrum. Because the green light in the middle of the visible region is not efficiently absorbed, most of it is reflected into our eyes and gives plants their characteristic green color.

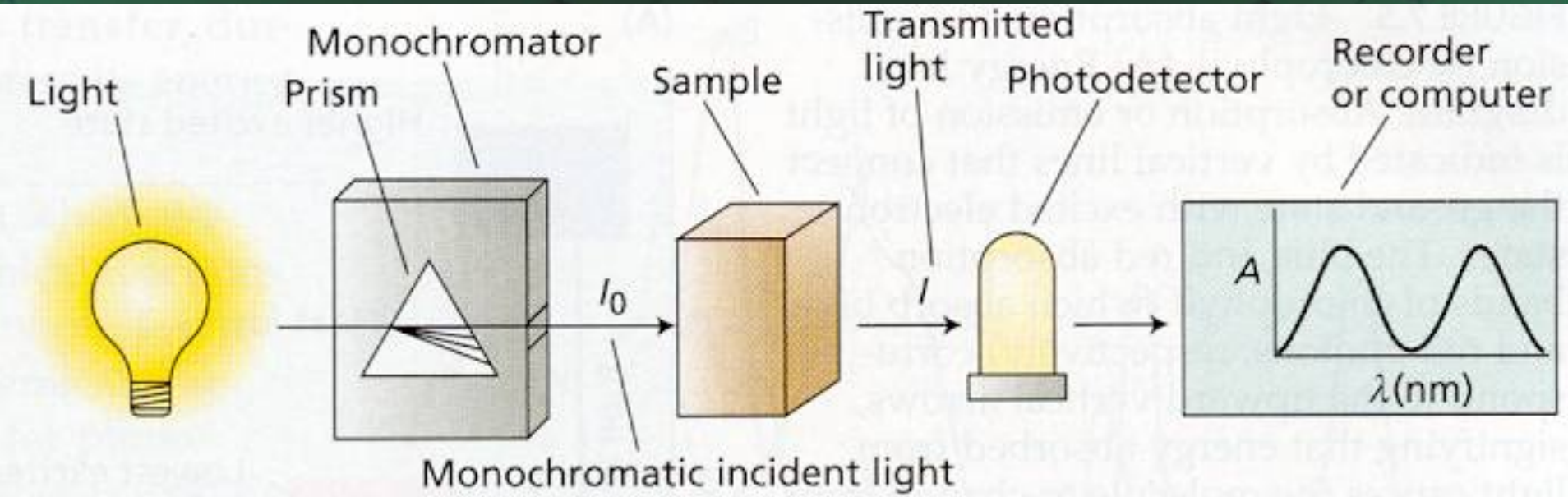

FIGURE 7.4 Schematic diagram of a spectrophotometer. The instrument consists of a light source, a monochromator that contains a wavelength selection device such as a prism, a sample holder, a photodetector, and a recorder or computer. The output wavelength of the monochromator can be changed by rotation of the prism; the graph of absorbance (A) versus wavelength (λ) is called a spectrum.

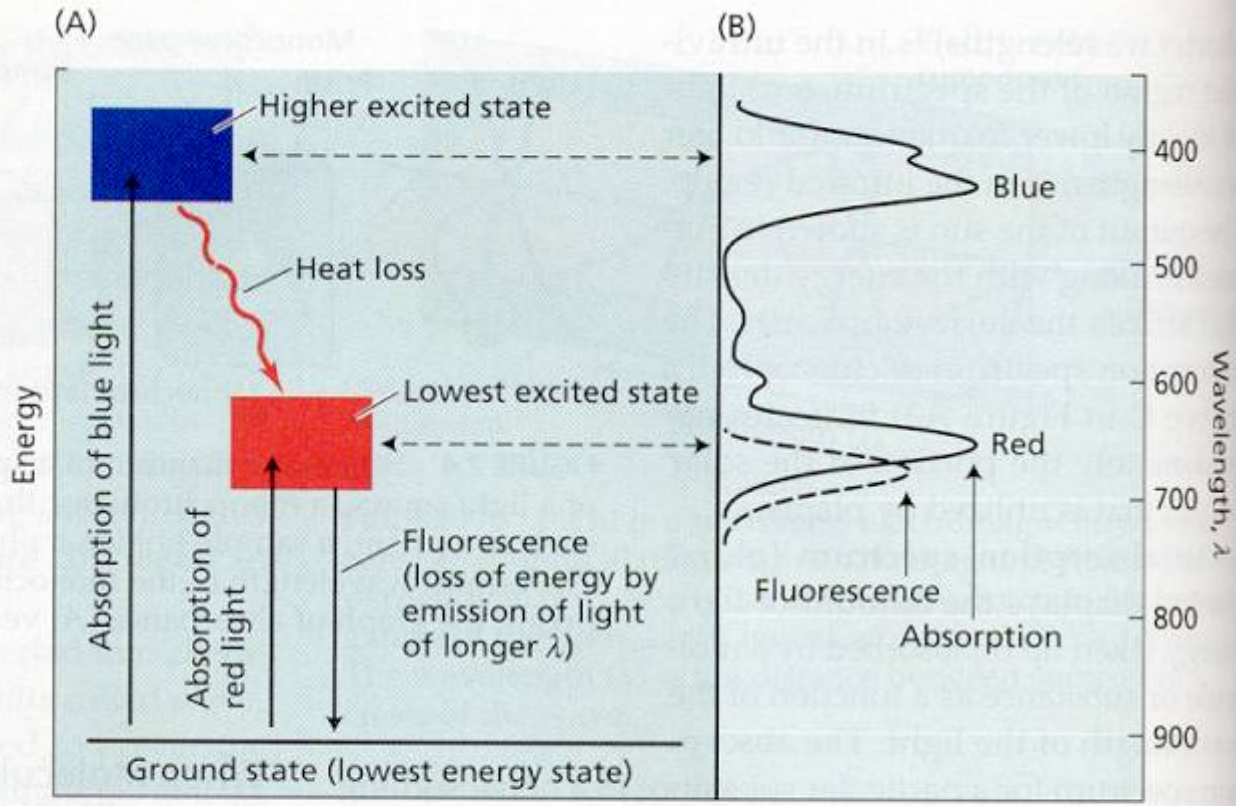

FIGURE 7.5 Light absorption and emission by chlorophyll. (A) Energy level diagram. Absorption or emission of light is indicated by vertical lines that connect the ground state with excited electron states. The blue and red absorption bands of chlorophyll (which absorb blue and red photons, respectively) correspond to the upward vertical arrows, signifying that energy absorbed from light causes the molecule to change from the ground state to an excited state. The downward-pointing arrow indicates fluorescence, in which the molecule goes from the lowest excited state to the ground state while re-emitting energy as a photon. (B) Spectra of absorption and fluorescence. The long-wavelength (red) absorption band of chlorophyll corresponds to light that has the energy required to cause the transition from the ground state to the first excited state. The short-wavelength (blue) absorption band corresponds to a transition to a higher excited state.

(A) **Chlorophylls**

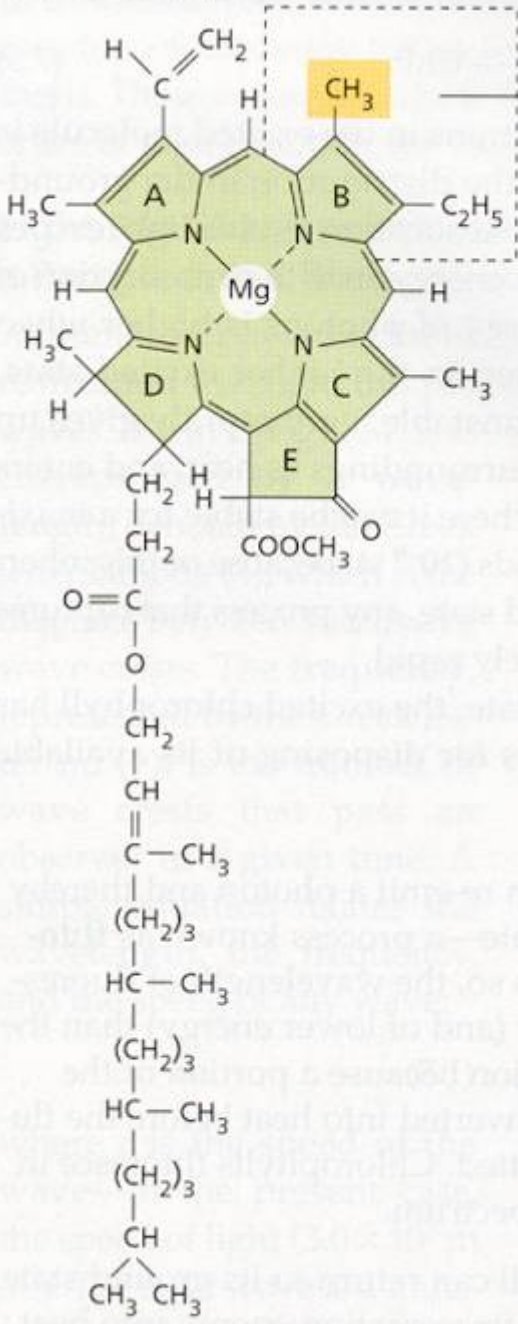

Chlorophyll *a*

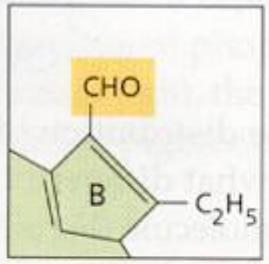

Chlorophyll *b*

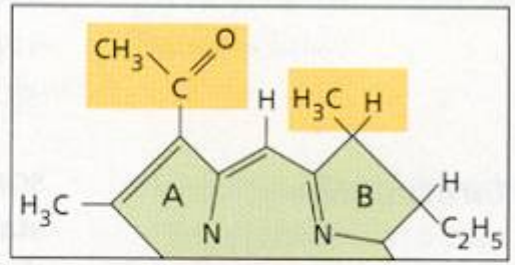

Bacteriochlorophyll *a*

(B) **Carotenoids**

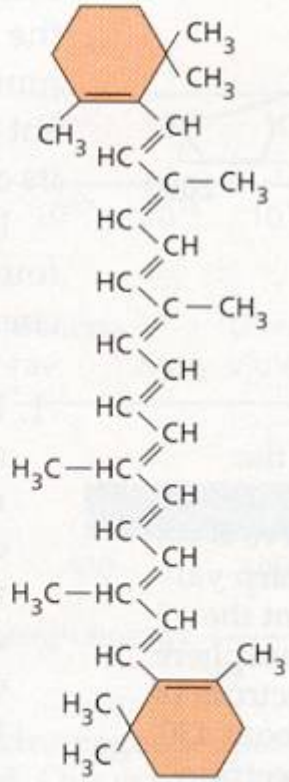

β-Carotene

(C) **Bilin pigments**

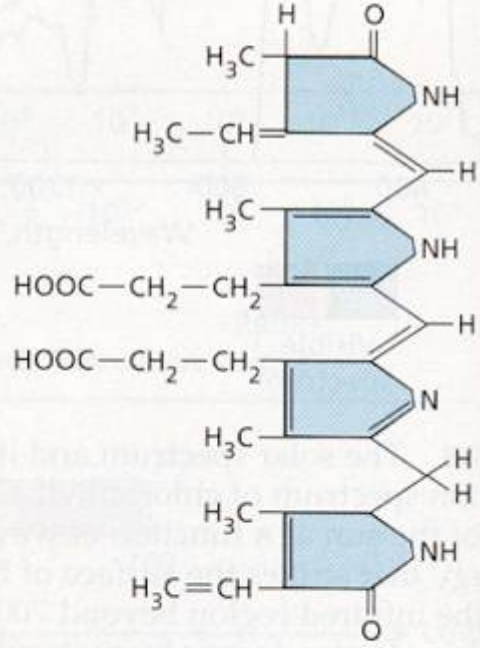

Phycoerythrobilin

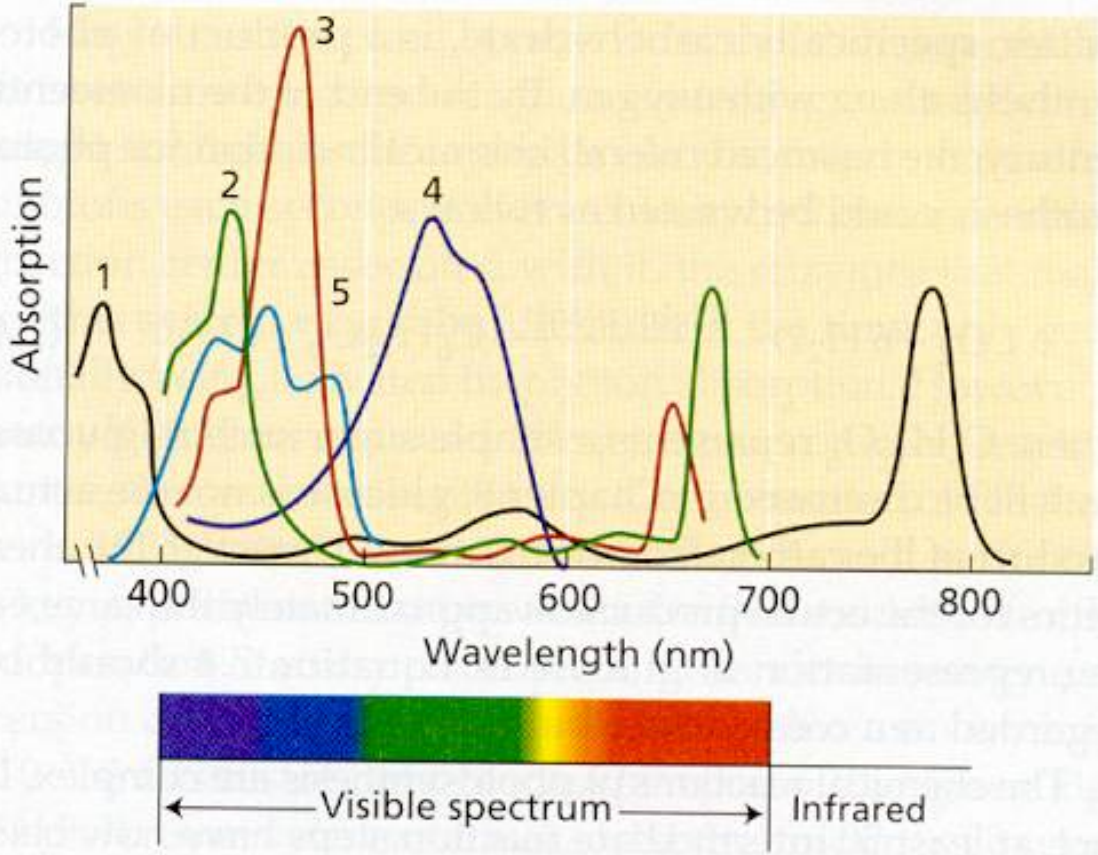

FIGURE 7.7 Absorption spectra of some photosynthetic pigments. Curve 1, bacteriochlorophyll *a*; curve 2, chlorophyll *a*; curve 3, chlorophyll *b*; curve 4, phycoerythrobilin; curve 5, β-carotene. The absorption spectra shown are for pure pigments dissolved in nonpolar solvents, except for curve 4, which represents an aqueous buffer of phycoerythrin, a protein from cyanobacteria that contains a phycoerythrobilin chromophore covalently attached to the peptide chain. In many cases the spectra of photosynthetic pigments in vivo are substantially affected by the environment of the pigments in the photosynthetic membrane. (After Avers 1985.)

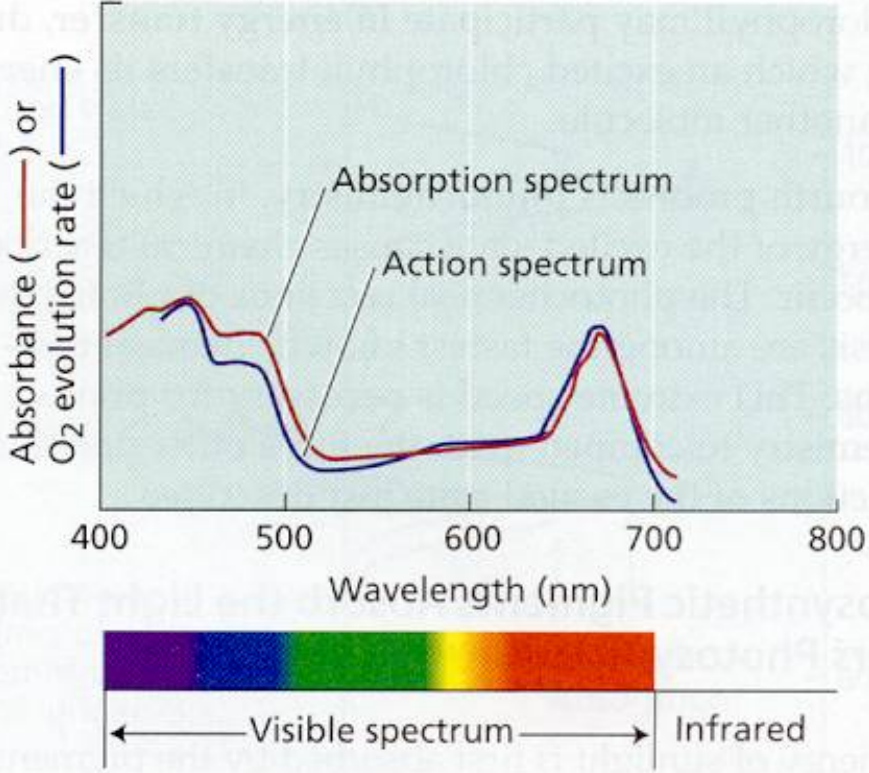

FIGURE 7.8 Action spectrum compared with an absorption spectrum. The absorption spectrum is measured as shown in Figure 7.4. An action spectrum is measured by plotting a response to light such as oxygen evolution, as a function of wavelength. If the pigment used to obtain the absorption spectrum is the same as those that cause the response, the absorption and action spectra will match. In the example shown here, the action spectrum for oxygen evolution matches the absorption spectrum of intact chloroplasts quit well, indicating that light absorption by the chlorophylls mediates oxygen evolution. Discrepancies are found in the region of carotenoid absorption, from 450 to 550 nm, indicating that energy transfer from carotenoids to chlorophylls is not as effective as energy transfer between chlorophylls.

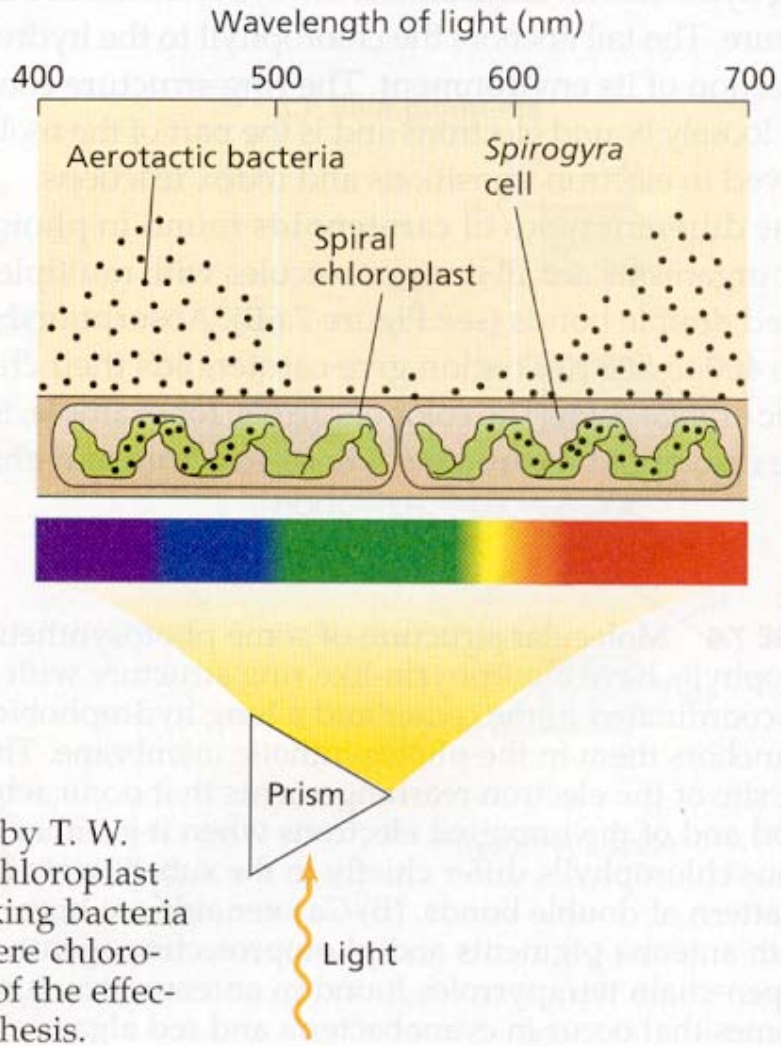

FIGURE 7.9 Schematic diagram of the action spectrum measurements by T. W. Engelmann. Engelmann projected a spectrum of light onto the spiral chloroplast of the filamentous green alga *Spirogyra* and observed that oxygen-seeking bacteria introduced into the system collected in the region of the spectrum where chlorophyll pigments absorb. This action spectrum gave the first indication of the effectiveness of light absorbed by accessory pigments in driving photosynthesis.

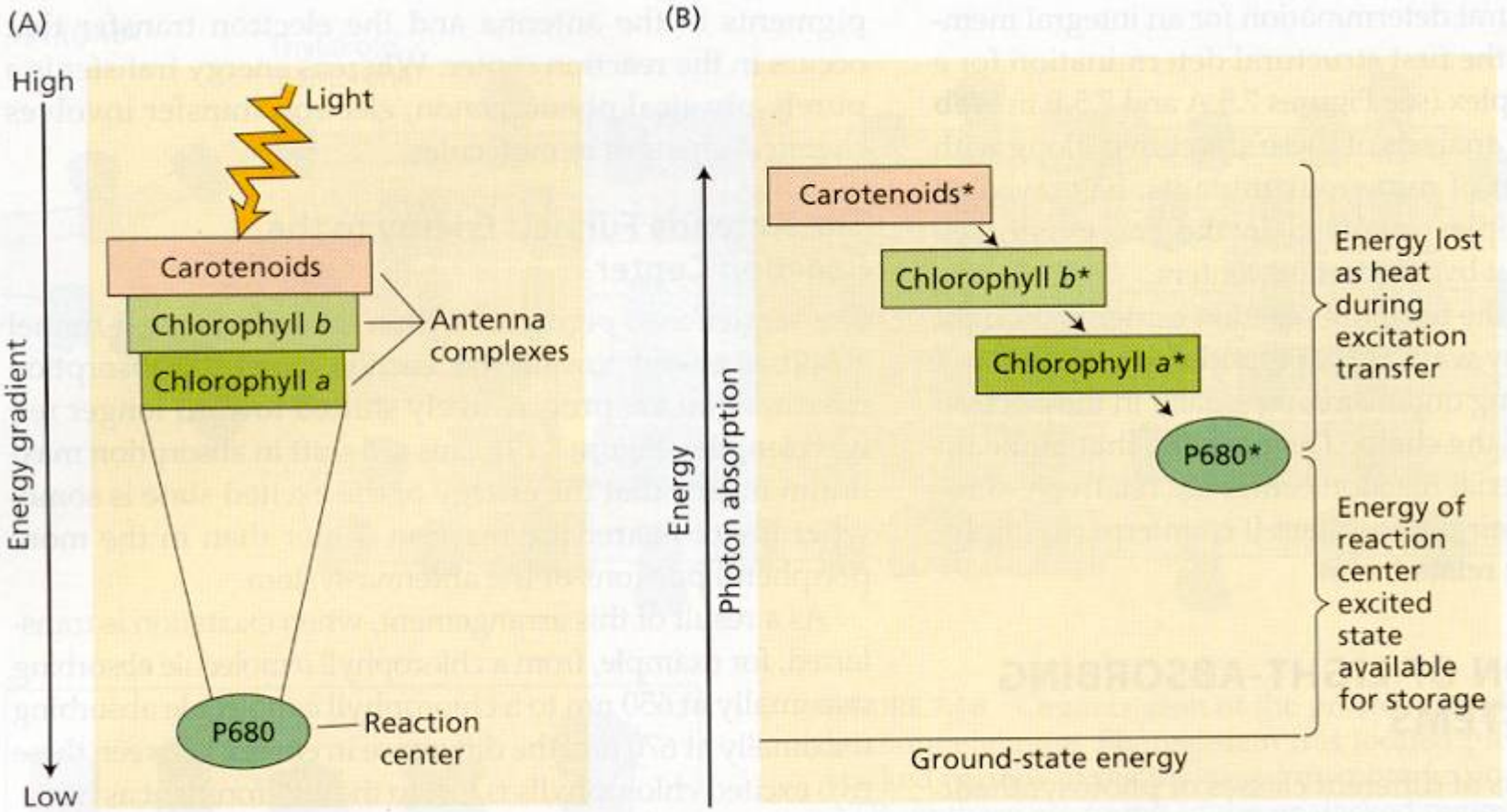

FIGURE 7.19 Funneling of excitation from the antenna system toward the reaction center. (A) The excited-state energy of pigments increases with distance from the reaction center; that is, pigments closer to the reaction center are lower in energy than those farther from the reaction center. This energy gradient ensures that excitation transfer toward the reaction center is energetically favorable and that excitation transfer back out to the peripheral portions of the antenna is energetically unfavorable. (B) Some energy is lost as heat to the environment by this process, but under optimal conditions almost all the excitations absorbed in the antenna complexes can be delivered to the reaction center. The asterisks denote an excited state.

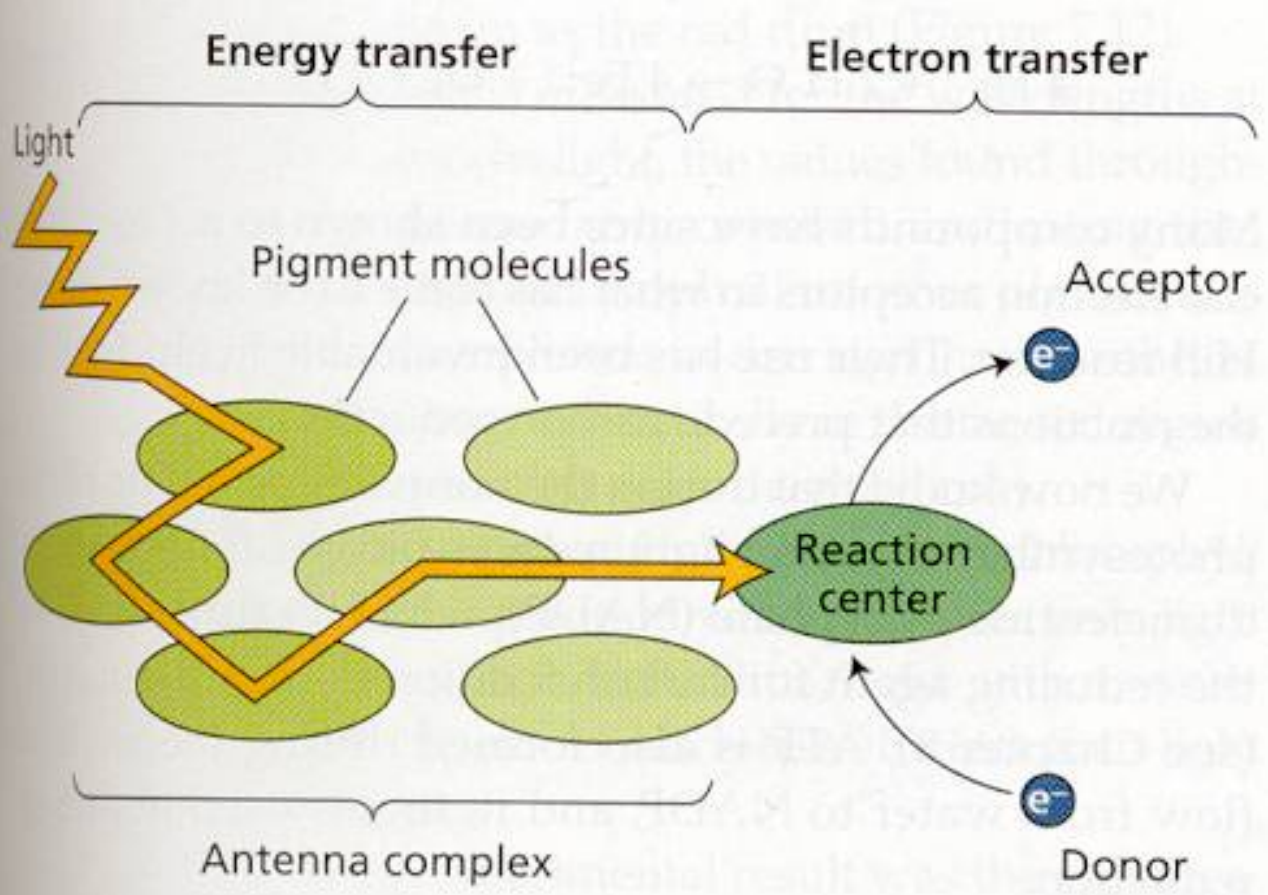

FIGURE 7.10 Basic concept of energy transfer during photosynthesis. Many pigments together serve as an antenna, collecting light and transferring its energy to the reaction center, where chemical reactions store some of the energy by transferring electrons from a chlorophyll pigment to an electron acceptor molecule. An electron donor then reduces the chlorophyll again. The transfer of energy in the antenna is a purely physical phenomenon and involves no chemical changes.

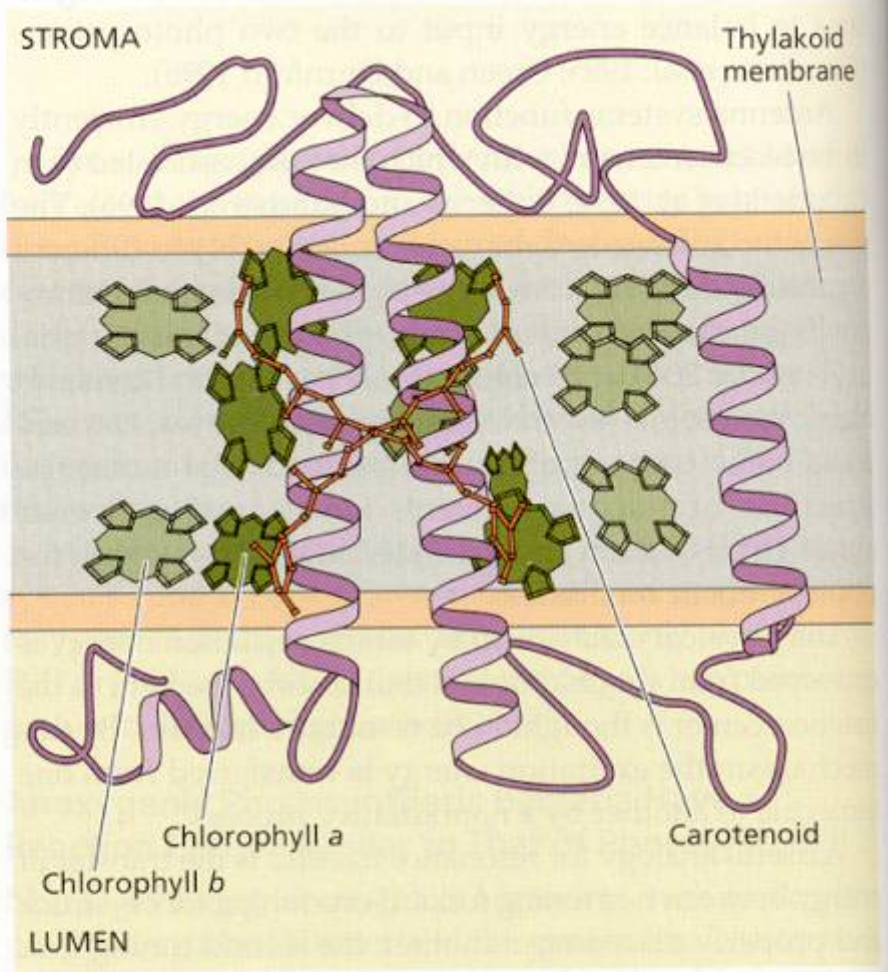

FIGURE 7.20 Two-dimensional view of the structure of the LHCII antenna complex from higher plants, determined by a combination of electron microscopy and electron crystallography. Like X-ray crystallography, electron crystallography uses the diffraction patterns of soft-energy electrons to resolve macromolecule structures. The antenna complex is a transmembrane pigment protein, with three helical regions that cross the nonpolar part of the membrane. Approximately 15 chlorophyll *a* and *b* molecules are associated with the complex, as well as several carotenoids. The positions of several of the chlorophylls are shown, and two of the carotenoids form an X in the middle of the complex. In the membrane, the complex is trimeric and aggregates around the periphery of the PSII reaction center complex. (After Kühlbrandt et al. 1994.)

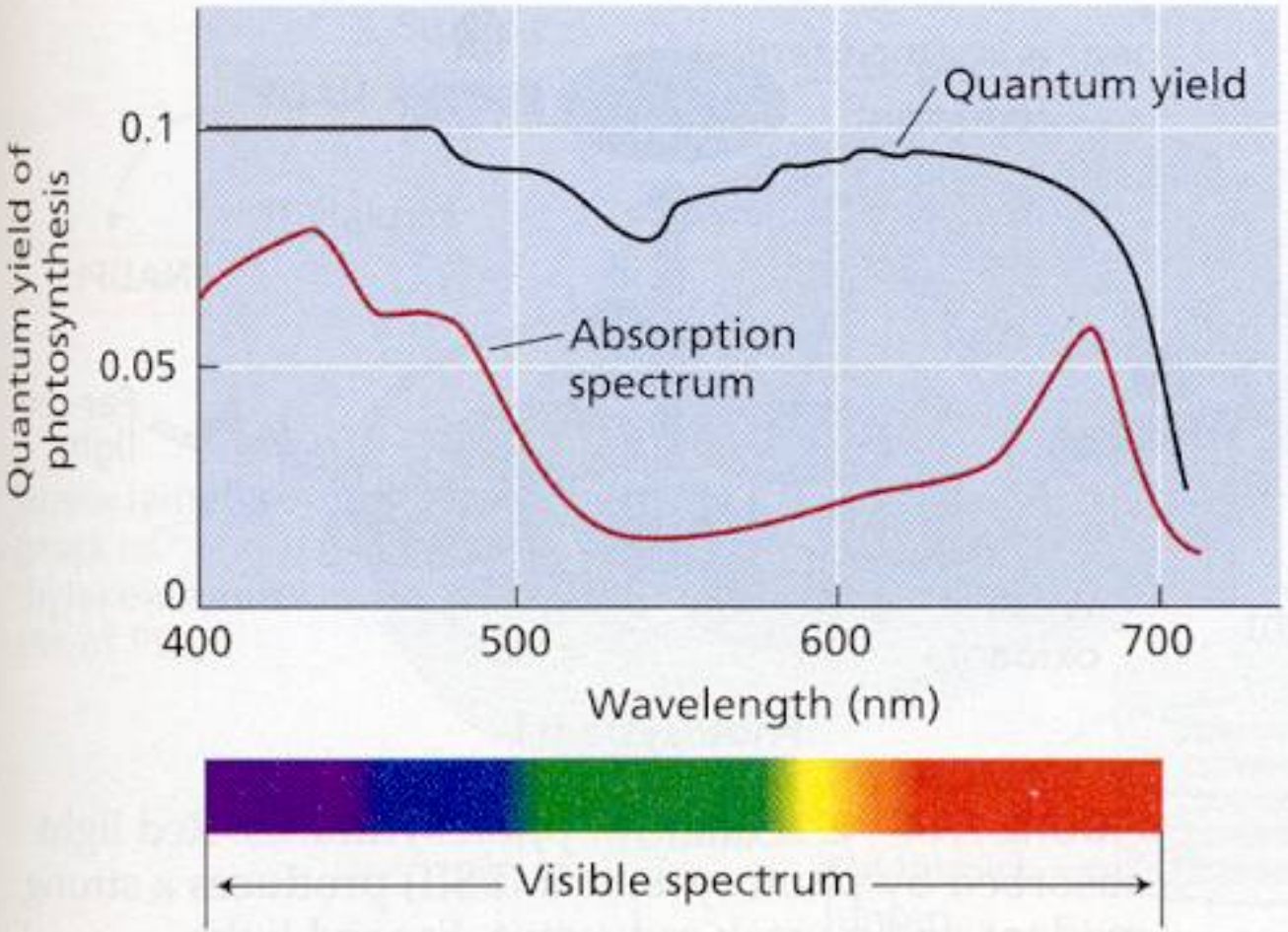

FIGURE 7.12 Red drop effect. The quantum yield of photosynthesis (black curve) falls off drastically for far-red light of wavelengths greater than 680 nm, indicating that far-red light alone is inefficient in driving photosynthesis. The slight dip near 500 nm reflects the somewhat lower efficiency of photosynthesis using light absorbed by accessory pigments, carotenoids.

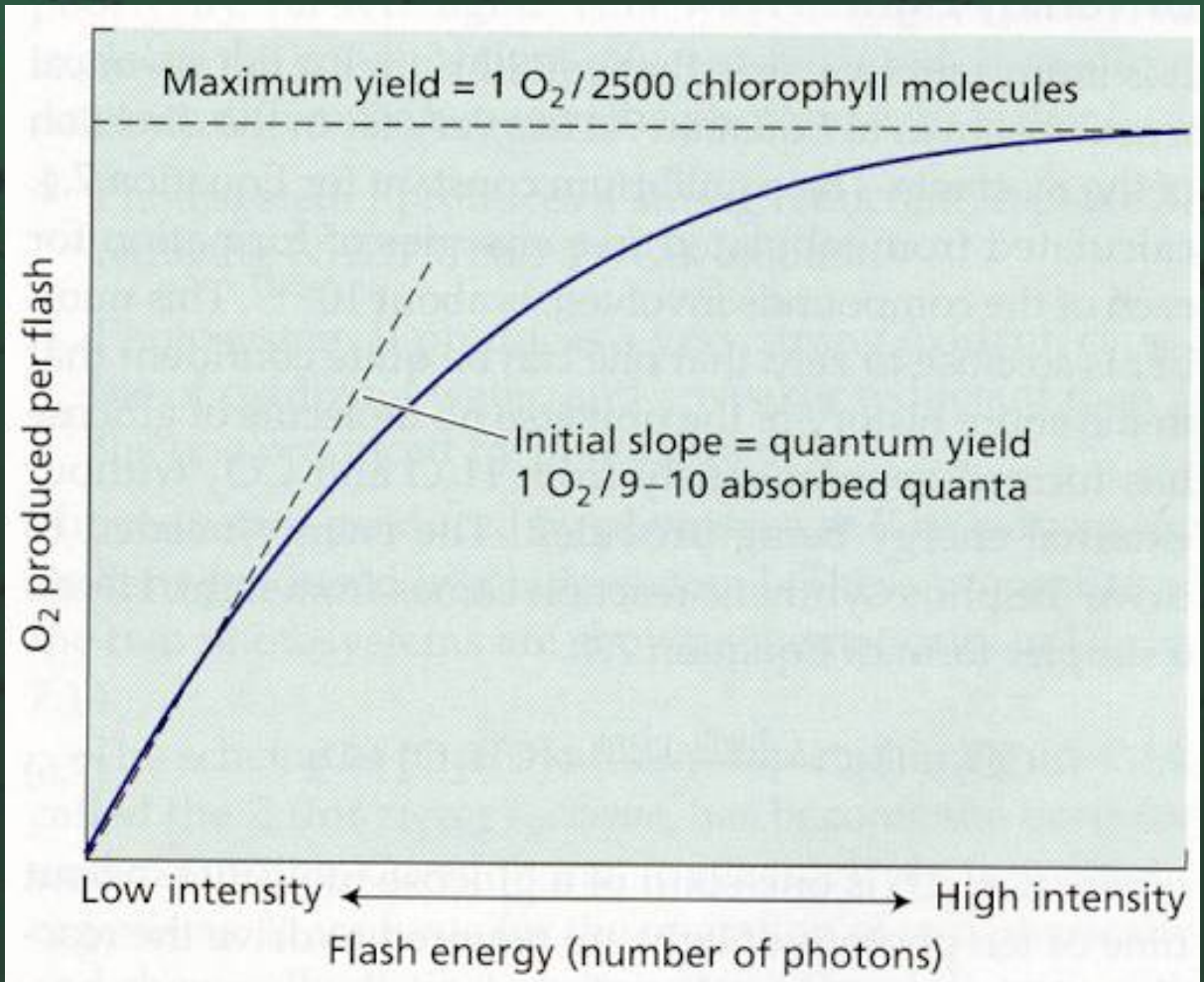

FIGURE 7.11 Relationship of oxygen production to flash energy, the first evidence for the interaction between the antenna pigments and the reaction center. At saturating energies, the maximum amount of O_2 produced is 1 molecule per 2500 chlorophyll molecules.

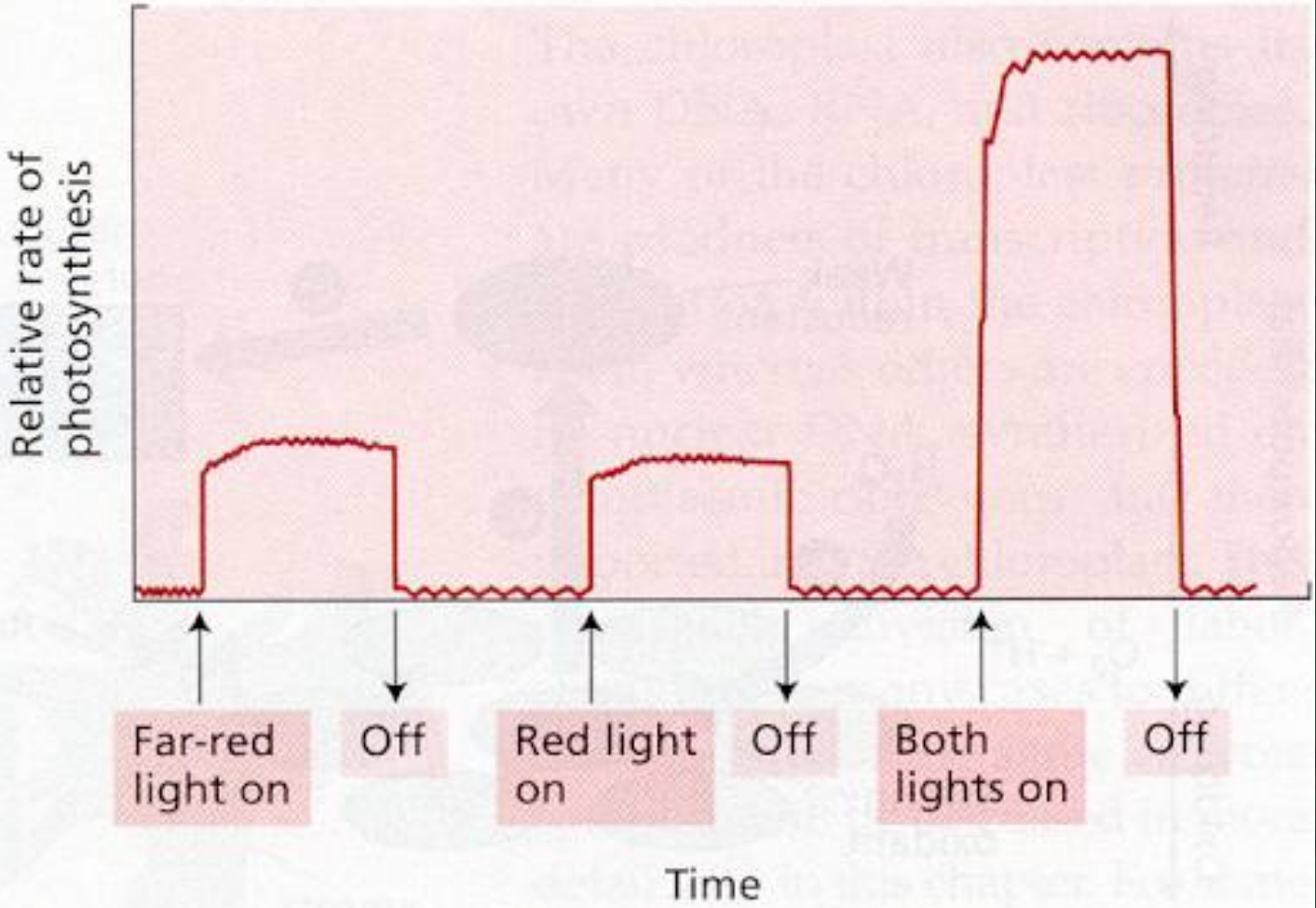

FIGURE 7.13 Enhancement effect. The rate of photosynthesis when red and far-red light are given together is greater than the sum of the rates when they are given apart. The enhancement effect provided essential evidence in favor of the concept that photosynthesis is carried out by two photochemical systems working in tandem but with slightly different wavelength optima.

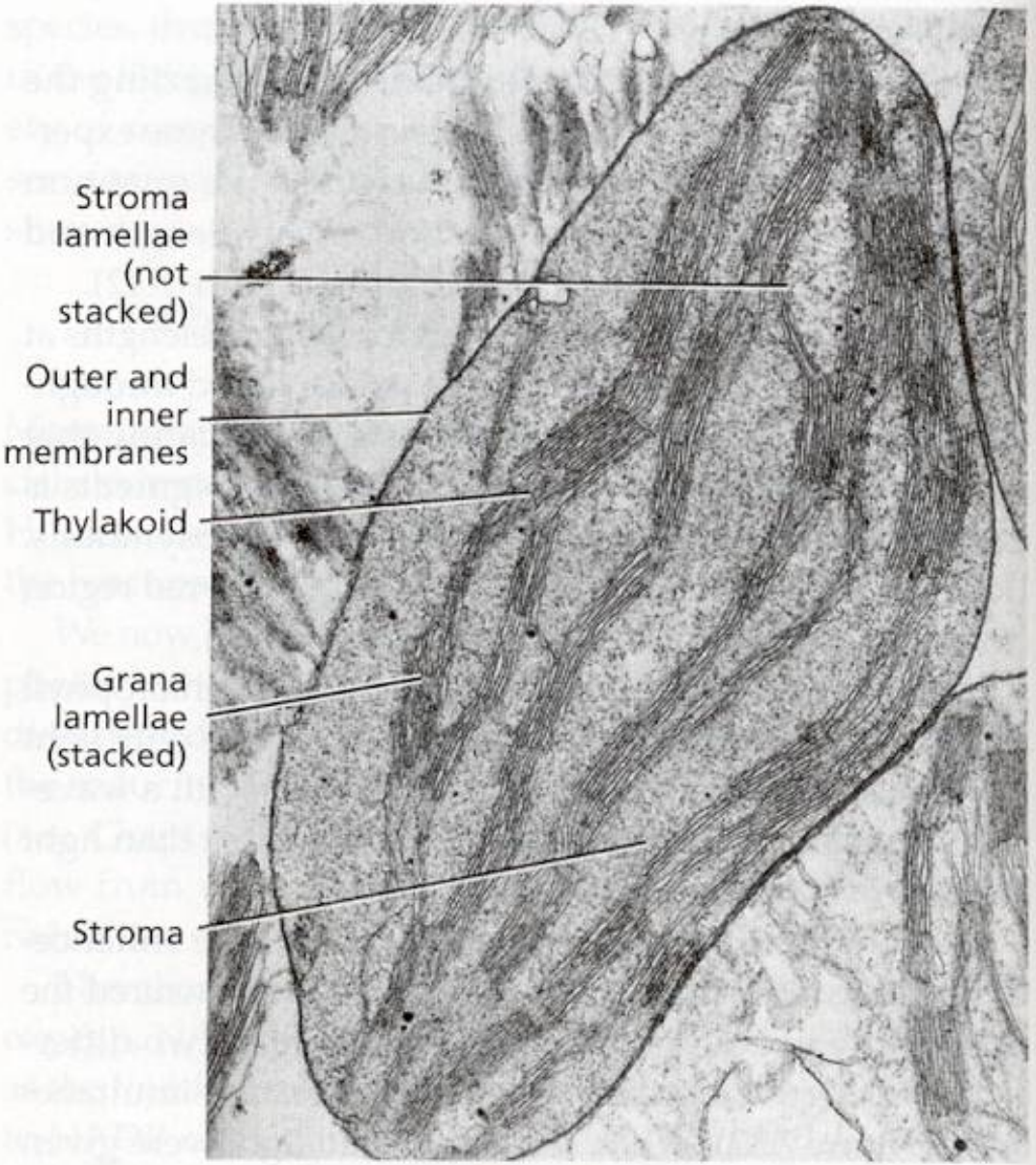

FIGURE 7.15 Transmission electron micrograph of a chloroplast from pea (*Pisum sativum*), fixed in glutaraldehyde and OsO_4, embedded in plastic resin, and thin-sectioned with an ultramicrotome. (14,500×) (Courtesy of J. Swafford.)

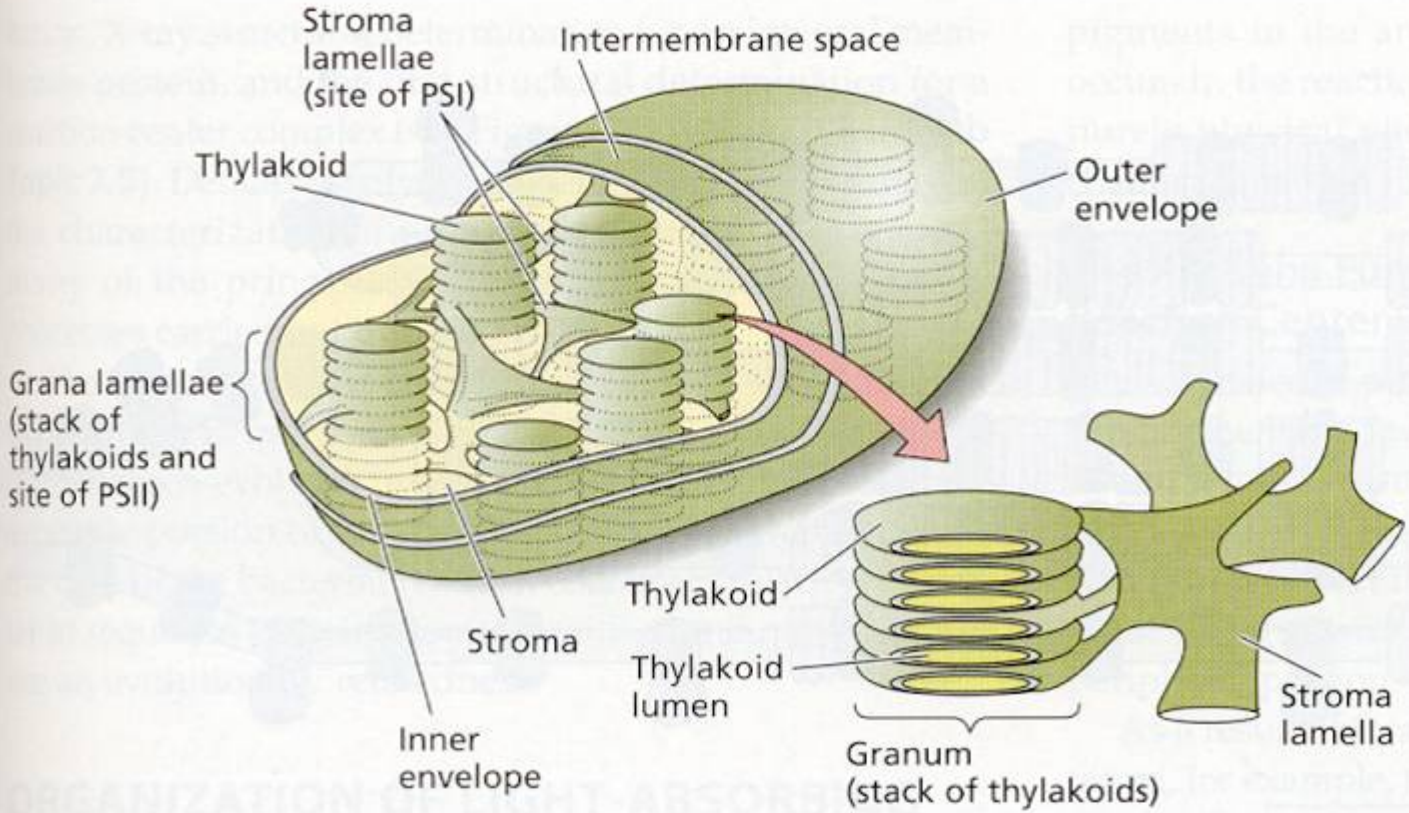

FIGURE 7.16 Schematic picture of the overall organization of the membranes in the chloroplast. The chloroplast of higher plants is surrounded by the inner and outer membranes (envelope). The region of the chloroplast that is inside the inner membrane and surrounds the thylakoid membranes is known as the stroma. It contains the enzymes that catalyze carbon fixation and other biosynthetic pathways. The thylakoid membranes are highly folded and appear in many pictures to be stacked like coins, although in reality they form one or a few large interconnected membrane systems, with a well-defined interior and exterior with respect to the stroma. The inner space within a thylakoid is known as the lumen. (After Becker 1986.)

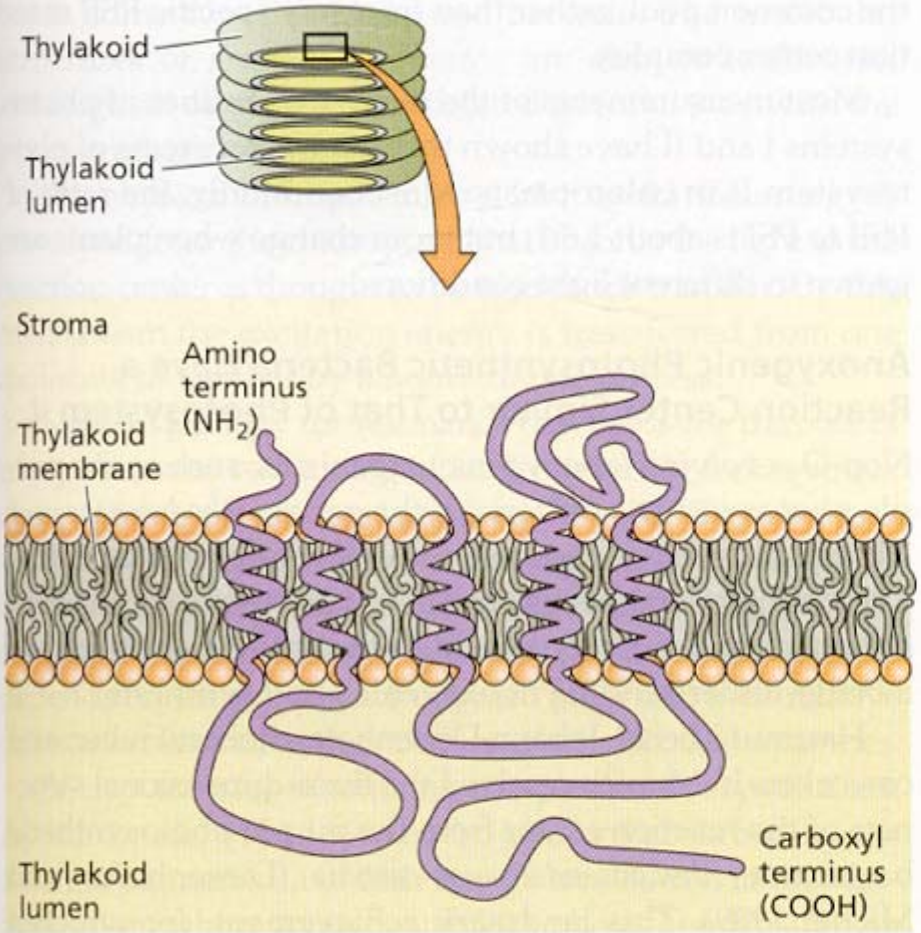

FIGURE 7.17 Predicted folding pattern of the D1 protein of the PSII reaction center. The hydrophobic portion of the membrane is traversed five times by the peptide chain rich in hydrophobic amino acid residues. The protein is asymmetrically arranged in the thylakoid membrane, with the amino (NH_2) terminus on the stromal side of the membrane and the carboxyl (COOH) terminus on the lumen side. (After Trebst 1986.)

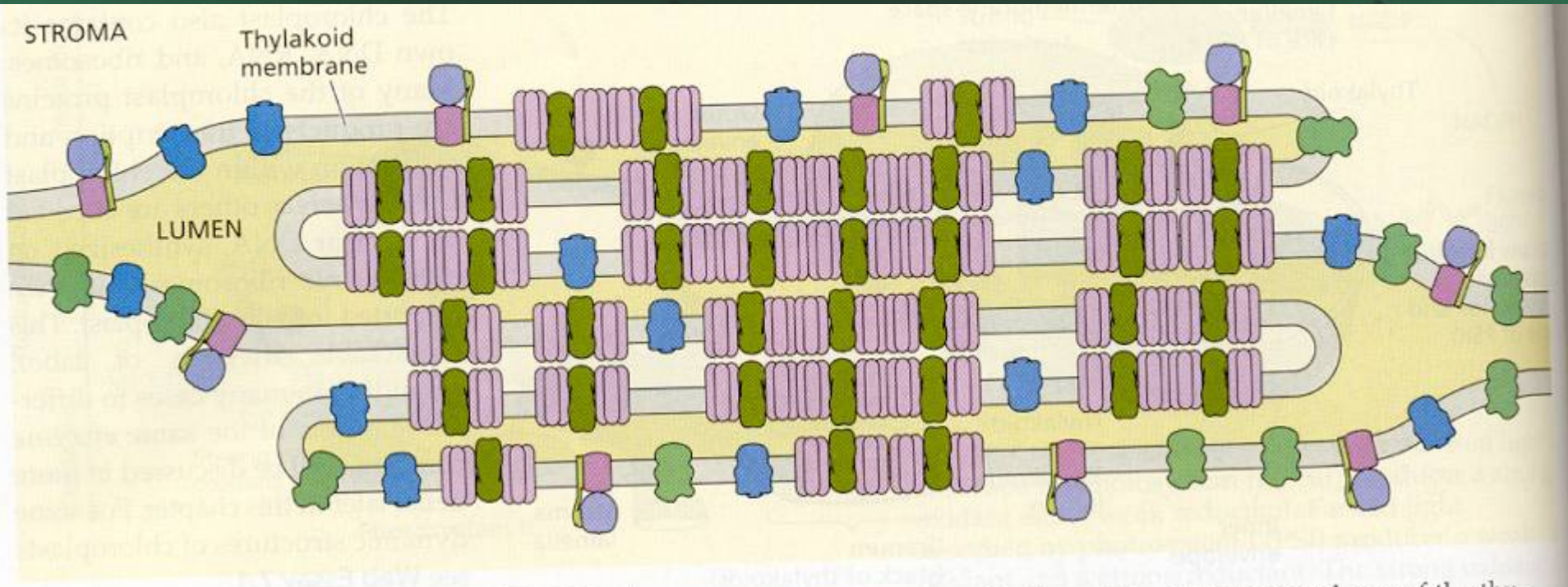

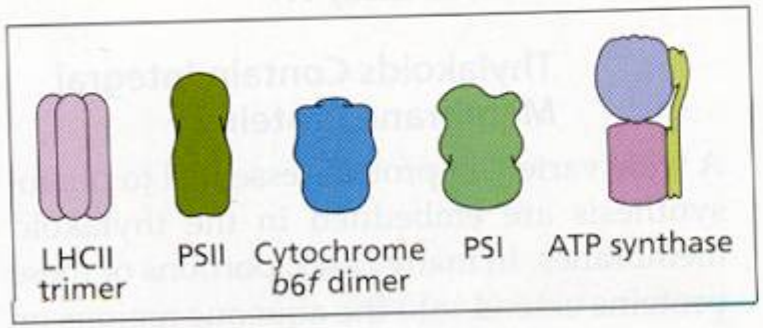

FIGURE 7.18 Organization of the protein complexes of the thylakoid membrane. Photosystem II is located predominantly in the stacked regions of the thylakoid membrane; photosystem I and ATP synthase are found in the unstacked regions protruding into the stroma. Cytochrome b_6f complexes are evenly distributed. This lateral separation of the two photosystems requires that electrons and protons produced by photosystem II be transported a considerable distance before they can be acted on by photosystem I and the ATP-coupling enzyme. (After Allen and Forsberg 2001.)

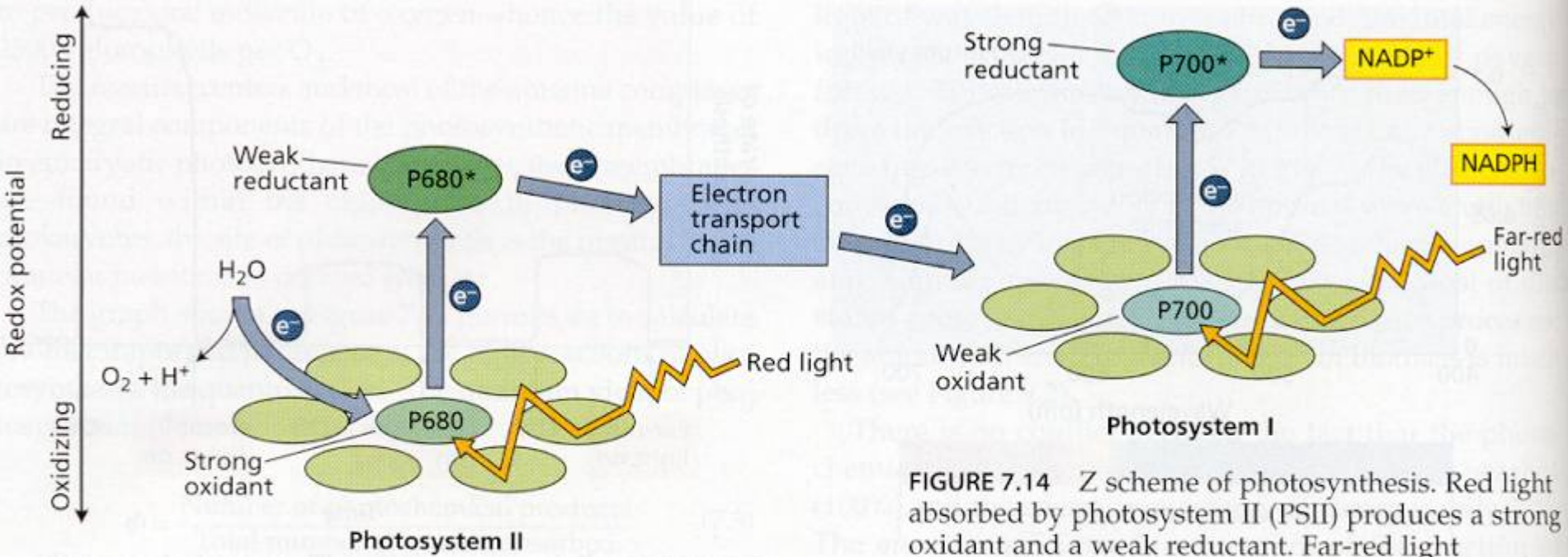

FIGURE 7.14 Z scheme of photosynthesis. Red light absorbed by photosystem II (PSII) produces a strong oxidant and a weak reductant. Far-red light absorbed by photosystem I (PSI) produces a weak oxidant and a strong reductant. The strong oxidant generated by PSII oxidizes water, while the strong reductant produced by PSI reduces $NADP^+$. This scheme is basic to an understanding of photosynthetic electron transport. P680 and P700 refer to the wavelengths of maximum absorption of the reaction center chlorophylls in PSII and PSI, respectively.

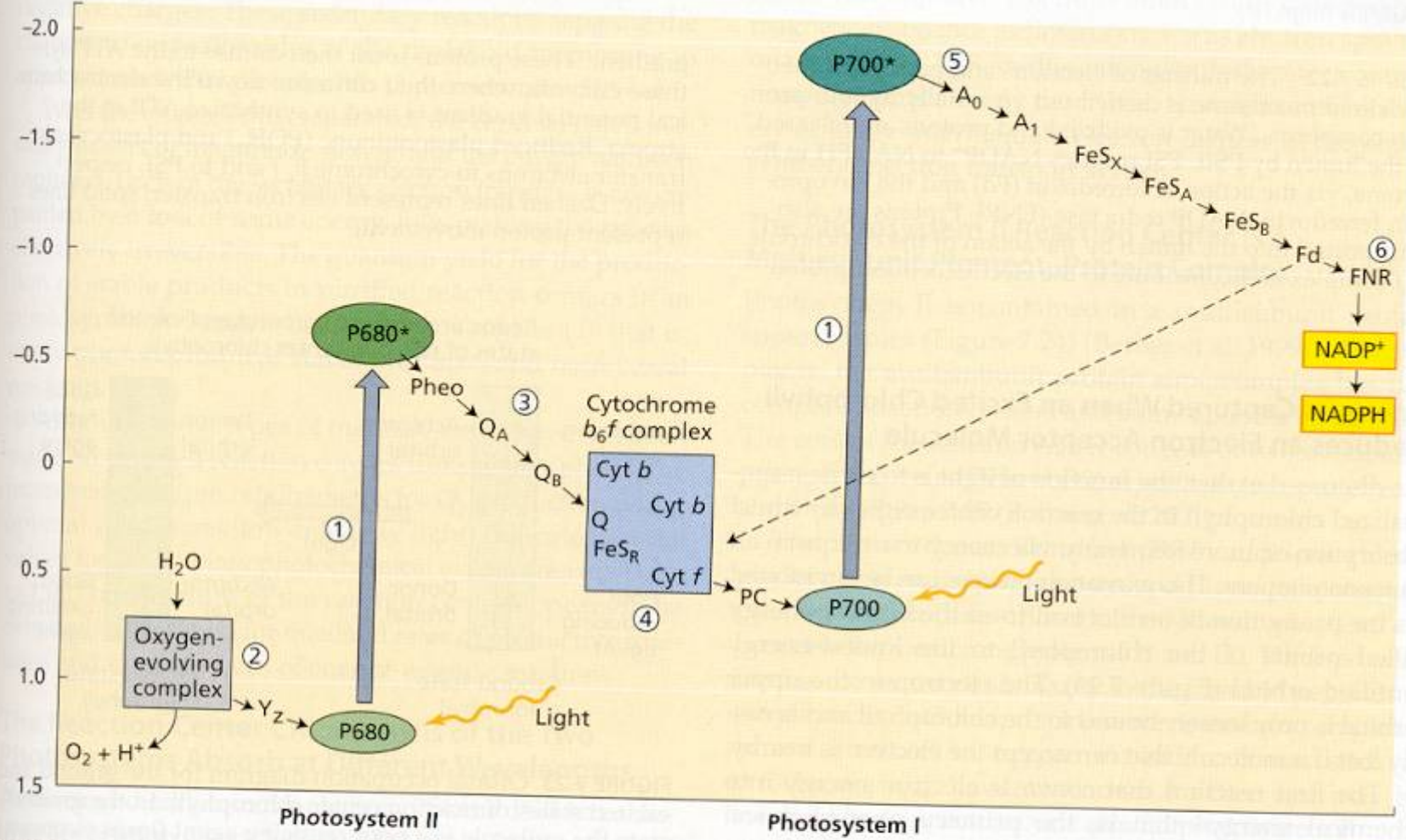

FIGURE 7.21 Detailed Z scheme for O_2-evolving photosynthetic organisms. The redox carriers are placed at their midpoint redox potentials (at pH 7). (1) The vertical arrows represent photon absorption by the reaction center chlorophylls: P680 for photosystem II (PSII) and P700 for photosystem I (PSI). The excited PSII reaction center chlorophyll, P680*, transfers an electron to pheophytin (Pheo). (2) On the oxidizing side of PSII (to the left of the arrow joining P680 with P680*), P680 oxidized by light is re-reduced by Y_z, that has received electrons from oxidation of water. (3) On the reducing side of PSII (to the right of the arrow joining P680 with P680*), pheophytin transfers electrons to the acceptors Q_A and Q_B, which are plastoquinones. (4) The cytochrome b_6f complex transfers electrons to plastocyanin (PC), a soluble protein, which in turn reduces $P700^+$ (oxidized P700). (5) The acceptor of electrons from P700* (A_0) is thought to be a chlorophyll, and the next acceptor (A_1) is a quinone. A series of membrane-bound iron–sulfur proteins (FeS_X, FeS_A, and FeS_B) transfers electrons to soluble ferredoxin (Fd). (6) The soluble flavoprotein ferredoxin–NADP reductase (FNR) reduces $NADP^+$ to NADPH, which is used in the Calvin cycle to reduce CO_2 (see Chapter 8). The dashed line indicates cyclic electron flow around PSI. (After Blankenship and Prince 1985.)

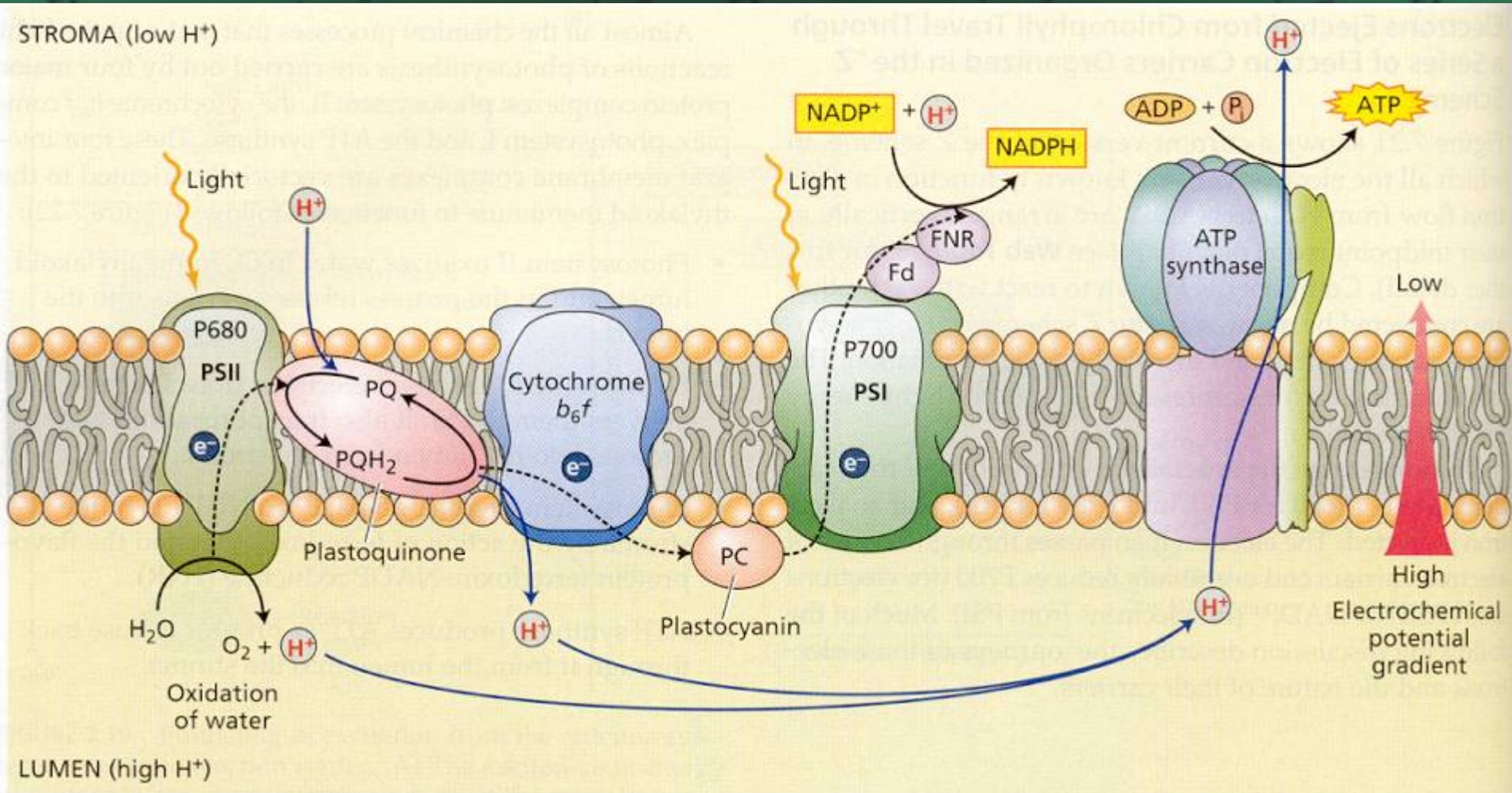

FIGURE 7.22 The transfer of electrons and protons in the thylakoid membrane is carried out vectorially by four protein complexes. Water is oxidized and protons are released in the lumen by PSII. PSI reduces $NADP^+$ to NADPH in the stroma, via the action of ferredoxin (Fd) and the flavoprotein ferredoxin–NADP reductase (FNR). Protons are also transported into the lumen by the action of the cytochrome b_6f complex and contribute to the electrochemical proton gradient. These protons must then diffuse to the ATP synthase enzyme, where their diffusion down the electrochemical potential gradient is used to synthesize ATP in the stroma. Reduced plastoquinone (PQH_2) and plastocyanin transfer electrons to cytochrome b_6f and to PSI, respectively. Dashed lines represent electron transfer; solid lines represent proton movement.

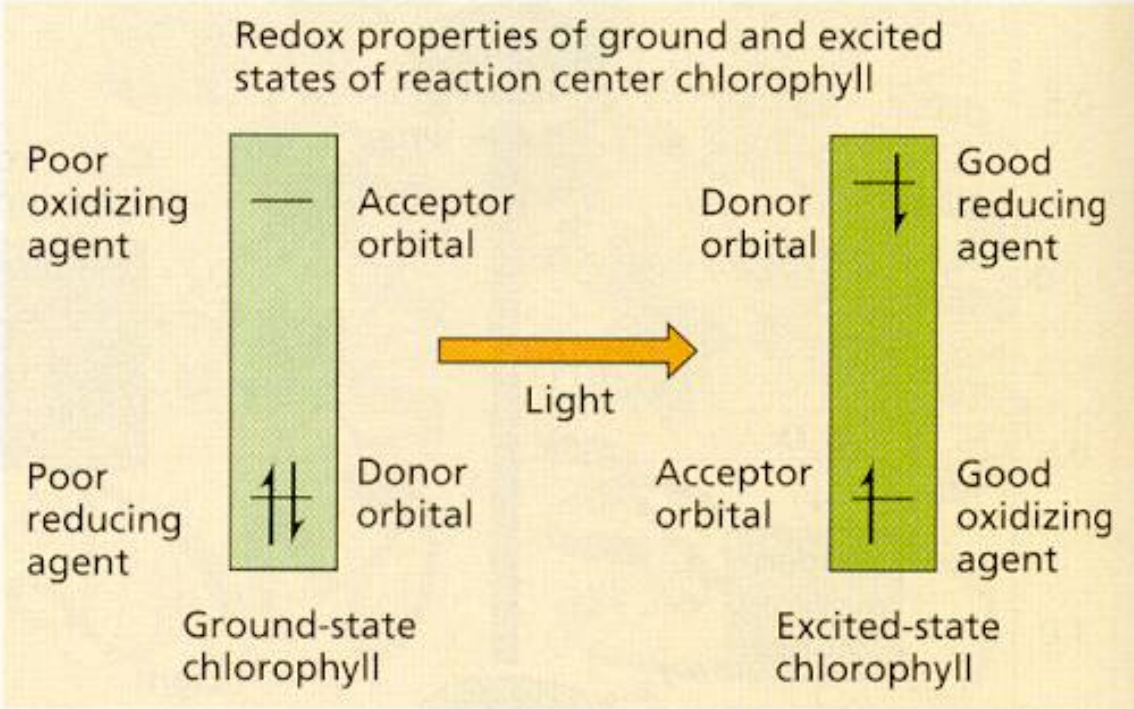

FIGURE 7.23 Orbital occupation diagram for the ground and excited states of reaction center chlorophyll. In the ground state the molecule is a poor reducing agent (loses electrons from a low-energy orbital) and a poor oxidizing agent (accepts electrons only into a high-energy orbital). In the excited state the situation is reversed, and an electron can be lost from the high-energy orbital, making the molecule an extremely powerful reducing agent. This is the reason for the extremely negative excited-state redox potential shown by P680* and P700* in Figure 7.21. The excited state can also act as a strong oxidant by accepting an electron into the lower-energy orbital, although this pathway is not significant in reaction centers. (After Blankenship and Prince 1985.)

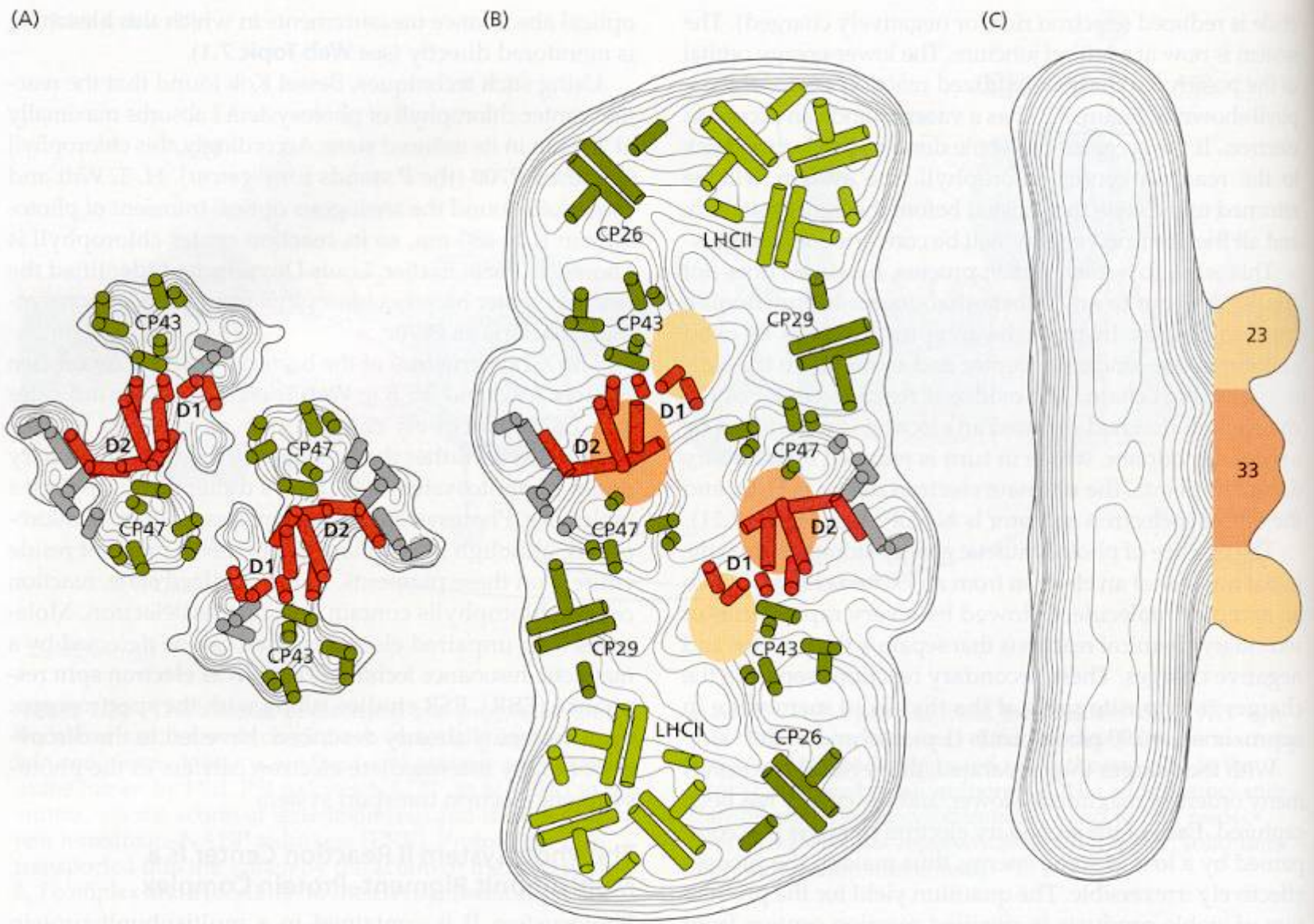

FIGURE 7.24 Structure of dimeric multisubunit protein supercomplex of photosystem II from higher plants, as determined by electron microscopy. The figure shows two complete reaction centers, each of which is a dimeric complex. (A) Helical arrangement of the D1 and D2 (red) and CP43 and CP47 (green) core subunits. (B) View from the lumenal side of the supercomplex, including additional antenna complexes, LHCII, CP26 and CP29, and extrinsic oxygen-evolving complex, shown as orange and yellow circles. Unassigned helices are shown in gray. (C) Side view of the complex illustrating the arrangement of the extrinsic proteins of the oxygen-evolving complex. (After Barber et al. 1999.)

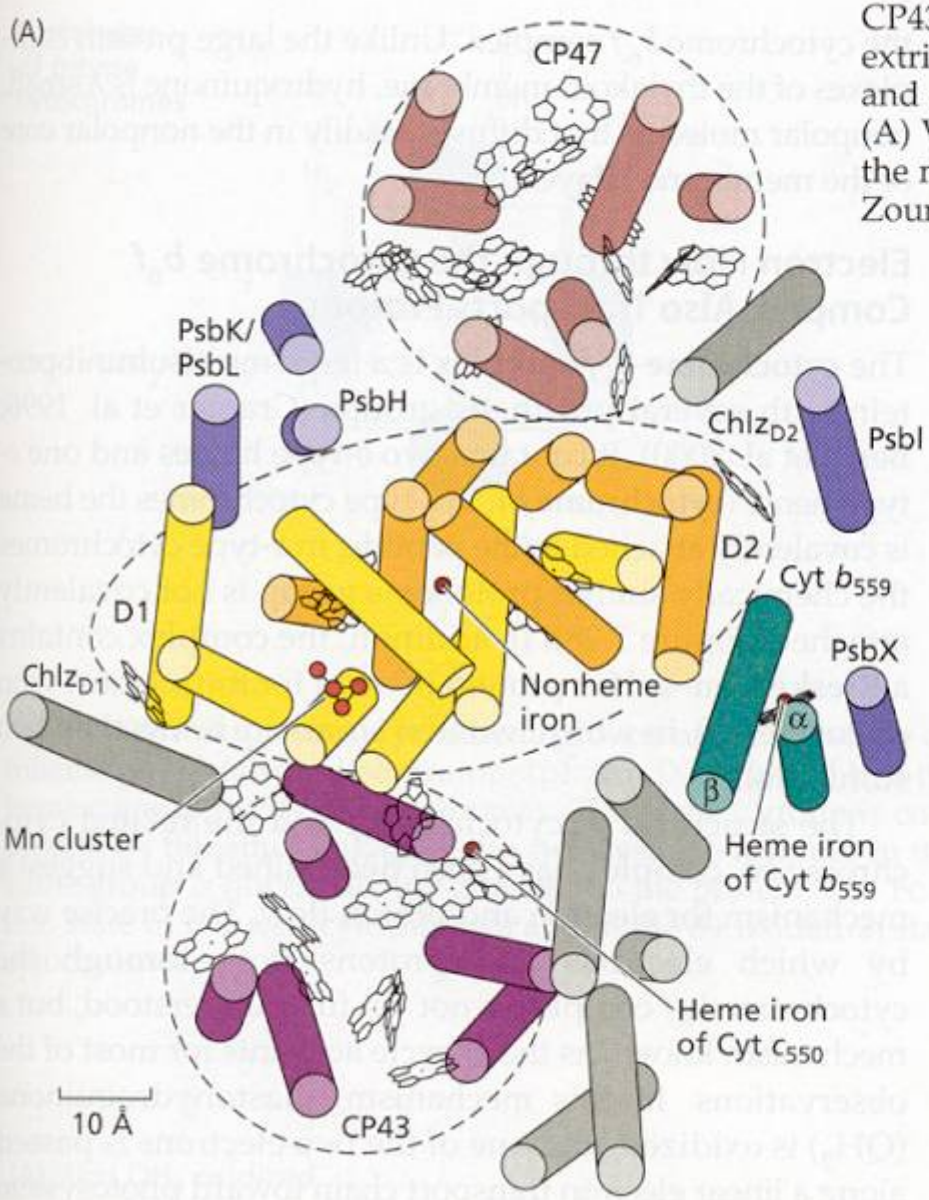

FIGURE 7.25 Structure of the photosystem II reaction center from the cyanobacterium *Synechococcus elongatus*, resolved at 3.8 Å. The structure includes the D1 and D1 core reaction center proteins, the CP43 and CP47 antenna proteins, cytochromes b_{559} and c_{550}, the extrinsic 33 kDa oxygen evolution protein PsbO, and the pigments and other cofactors. Seven unassigned helices are shown in gray. (A) View from the lumenal surface, perpendicular to the plane of the membrane. (B) Side view parallel to the membrane plane. (After Zouni et al. 2001.)

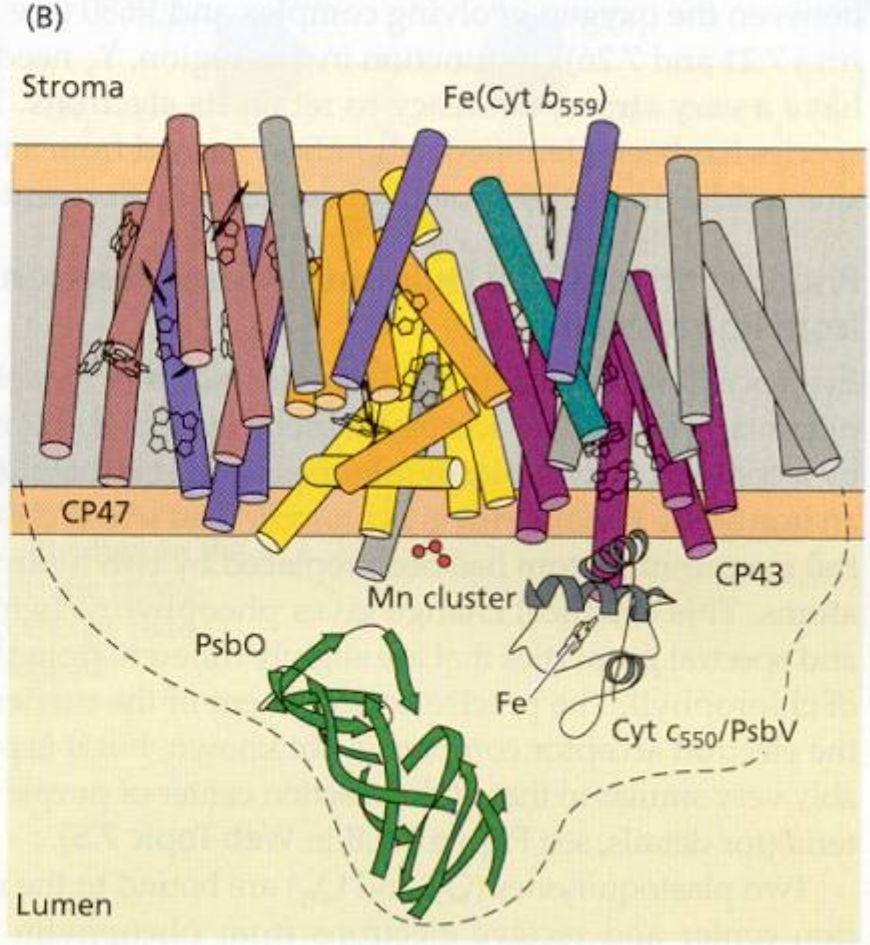

FIGURE 7.26 Model of the S state cycle of oxygen evolution in PSII. Successive stages in the oxidation of water via the Mn oxygen-evolving complex are shown. Y_z is a tyrosine radical that is an intermediate electron carrier between P680 and the Mn cluster. (After Tommos and Babcock 1998.)

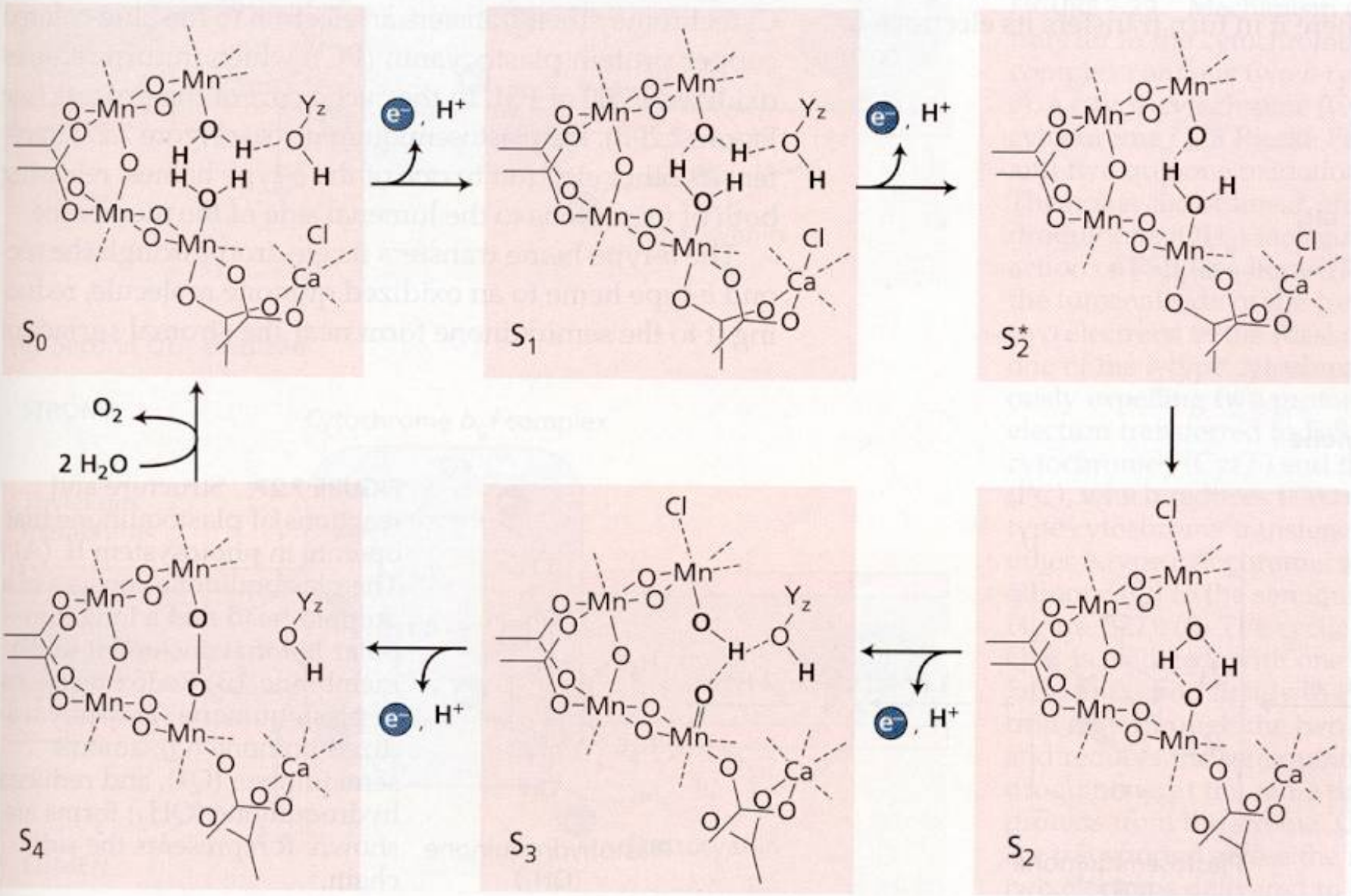

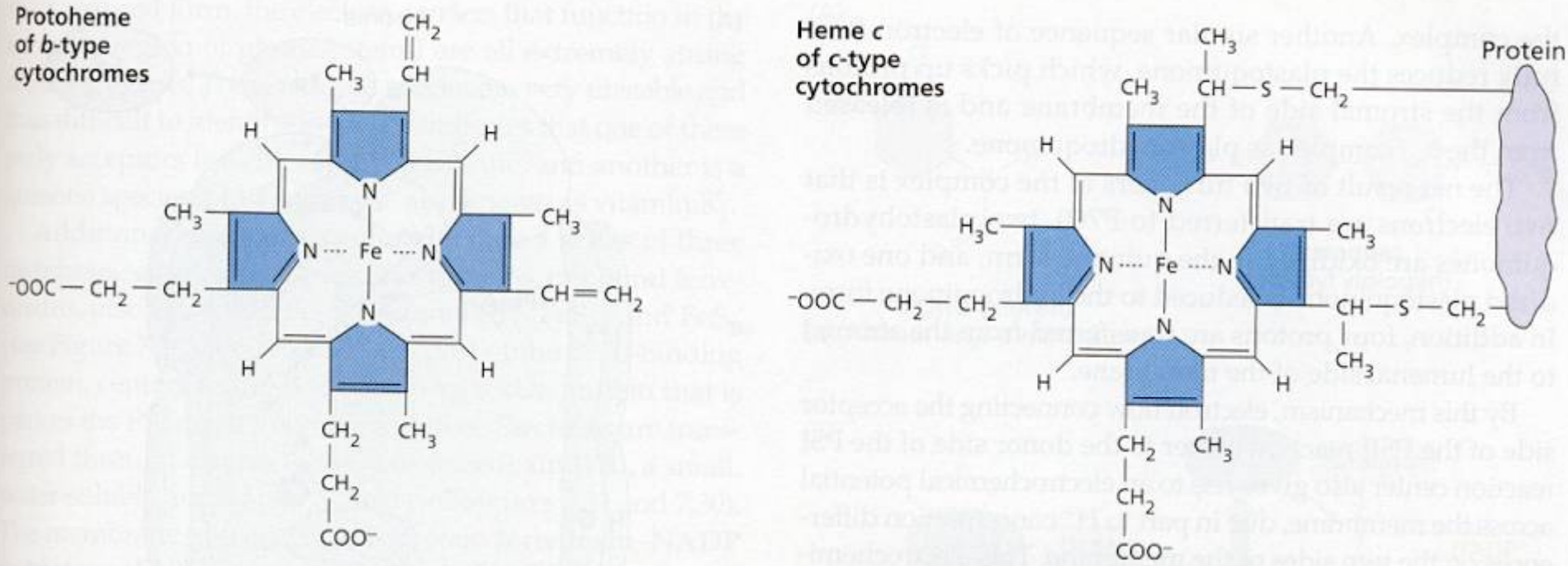

FIGURE 7.28 Structure of prosthetic groups of *b*- and *c*-type cytochromes. The protoheme group (also called protoporphyrin IX) is found in *b*-type cytochromes, the heme *c* group in *c*-type cytochromes. The heme *c* group is covalently attached to the protein by thioether linkages with two cysteine residues in the protein; the protoheme group is not covalently attached to the protein. The Fe ion is in the 2+ oxidation state in reduced cytochromes and in the 3+ oxidation state in oxidized cytochromes.

(A)

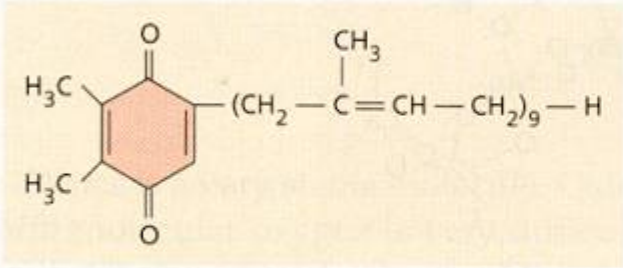

Plastoquinone

(B)

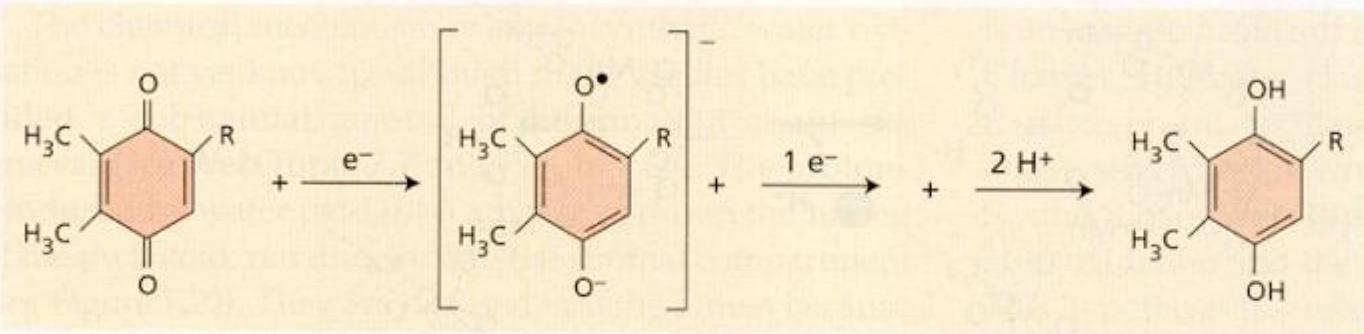

Quinone (Q)

Plastosemiquinone ($Q^{\bullet-}$)

Plastohydroquinone (QH_2)

FIGURE 7.27 Structure and reactions of plastoquinone tha operate in photosystem II. (A) The plastoquinone consists of quinoid head and a long non-polar tail that anchors it in the membrane. (B) Redox reaction of plastoquinone. The fully ox dized quinone (Q), anionic semiquinone ($Q^{\bullet-}$), and reduce hydroquinone (QH_2) forms ar shown; R represents the side chain.

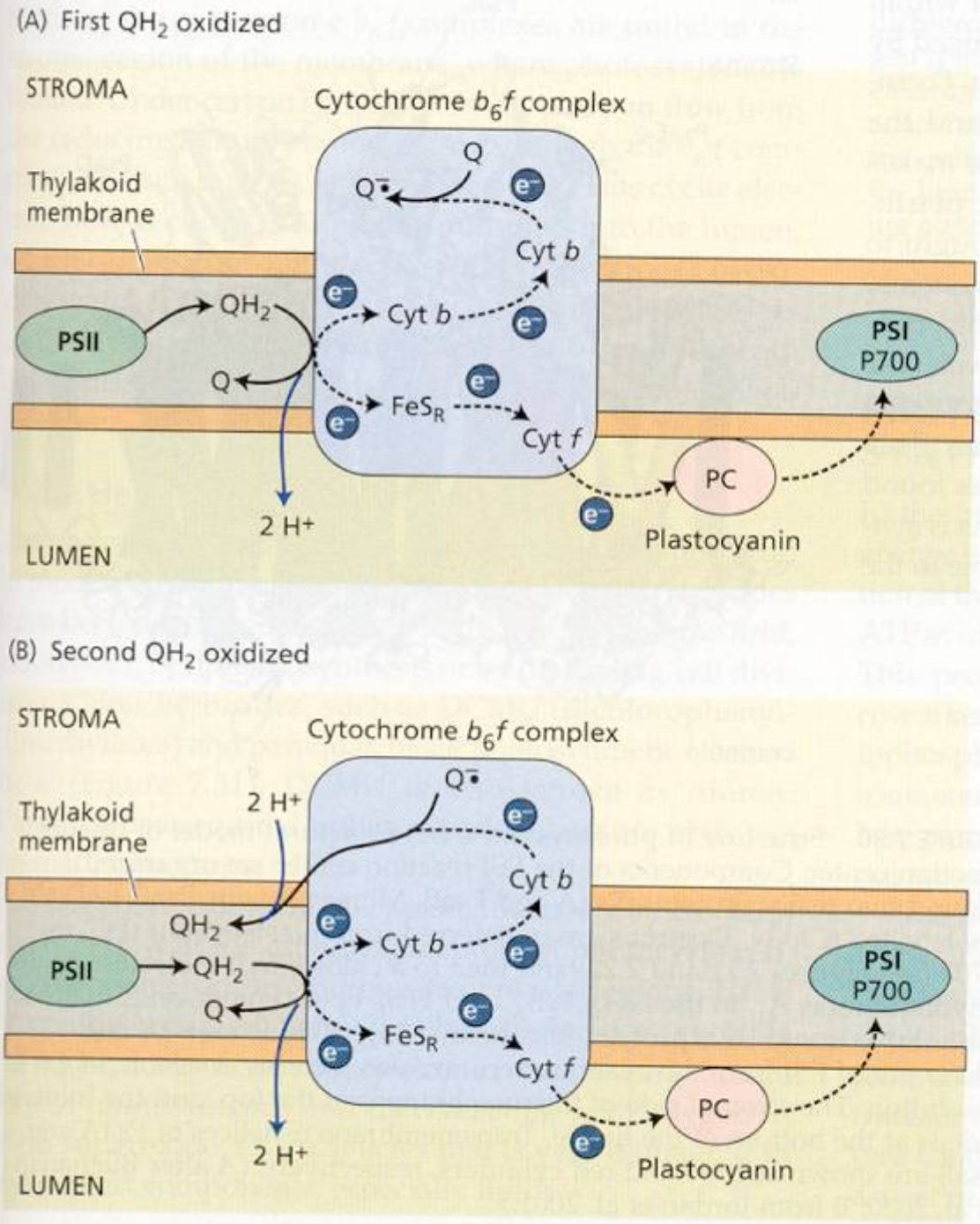

FIGURE 7.29 Mechanism of electron and proton transfer in the cytochrome b_6f complex. This complex contains two *b*-type cytochromes (Cyt *b*), a *c*-type cytochrome (Cyt *c*, historically called cytochrome *f*), a Rieske Fe–S protein (FeS_R), and two quinone oxidation–reduction sites. (A) The noncyclic or linear processes: A plastohydroquinone (QH_2) molecule produced by the action of PSII (see Figure 7.27) is oxidized near the lumenal side of the complex, transferring its two electrons to the Rieske Fe–S protein and one of the *b*-type cytochromes and simultaneously expelling two protons to the lumen. The electron transferred to FeS_R is passed to cytochrome *f* (Cyt *f*) and then to plastocyanin (PC), which reduces P700 of PSI. The reduced *b*-type cytochrome transfers an electron to the other *b*-type cytochrome, which reduces a quinone (Q) to the semiquinone ($Q^{\bullet}$) state (see Figure 7.27). (B) The cyclic processes: A second QH_2 is oxidized, with one electron going from FeS_R to PC and finally to P700. The second electron goes through the two *b*-type cytochromes and reduces the semiquinone to the plastohydroquinone, at the same time picking up two protons from the stroma. Overall, four protons are transported across the membrane for every two electrons delivered to P700.

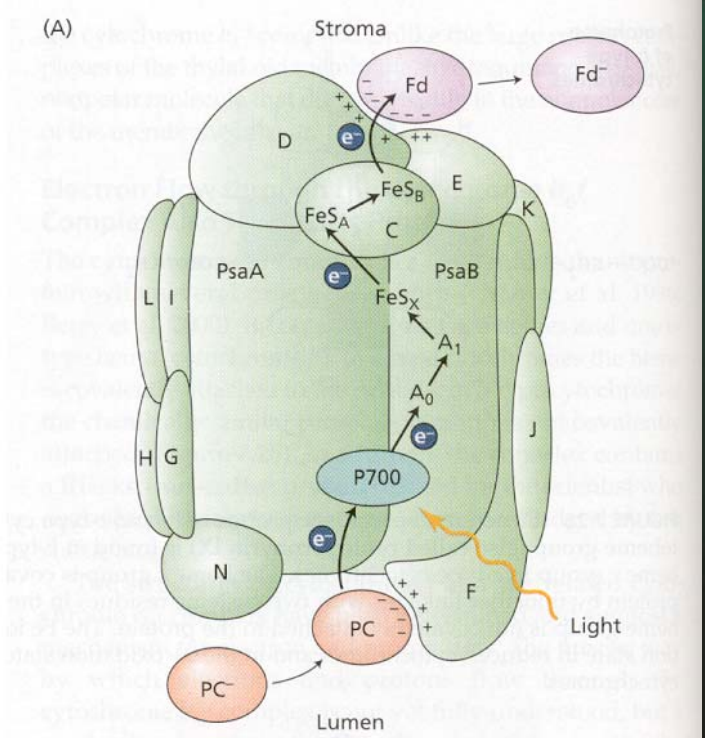

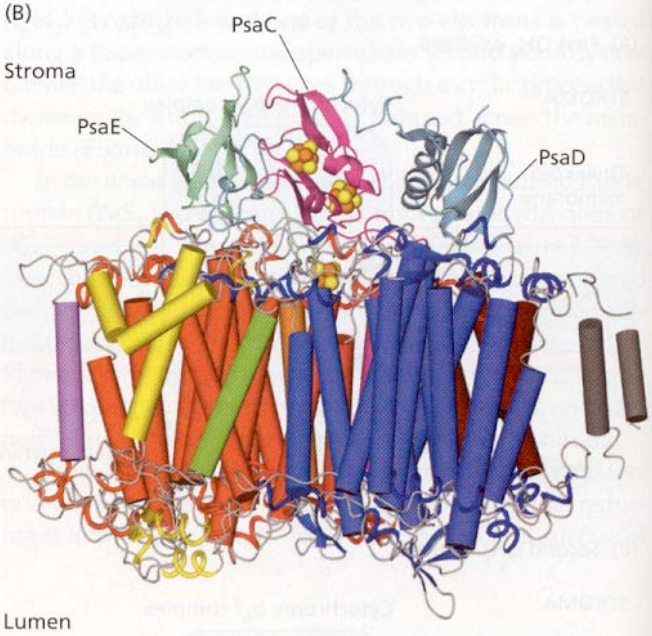

FIGURE 7.30 Structure of photosystem I. (A) Structural model of the PSI reaction center. Components of the PSI reaction center are organized around two major proteins, PsaA and PsaB. Minor proteins PsaC to PsaN are labelled C to N. Electrons are transferred from plastocyanin (PC) to P700 (see Figures 7.21 and 7.22) and then to a chlorophyll molecule, A_0, to phylloquinone, A_1, to the FeS_X, FeS_A, and FeS_B Fe–S centers, and finally to the soluble iron–sulfur protein, ferrodoxin (Fd). (B) Side view of one monomer of PSI from the cyanobacterium *Synechococcus elongatus*, at 2.5 Å resolution. The stromal side of the membrane is at the top, and the lumenal side is at the bottom of the figure. Transmembrane α-helices of PsaA and PsaB are shown as blue and red cylinders, respectively. (A after Buchanan et al. 2000; B from Jordan et al. 2001.)

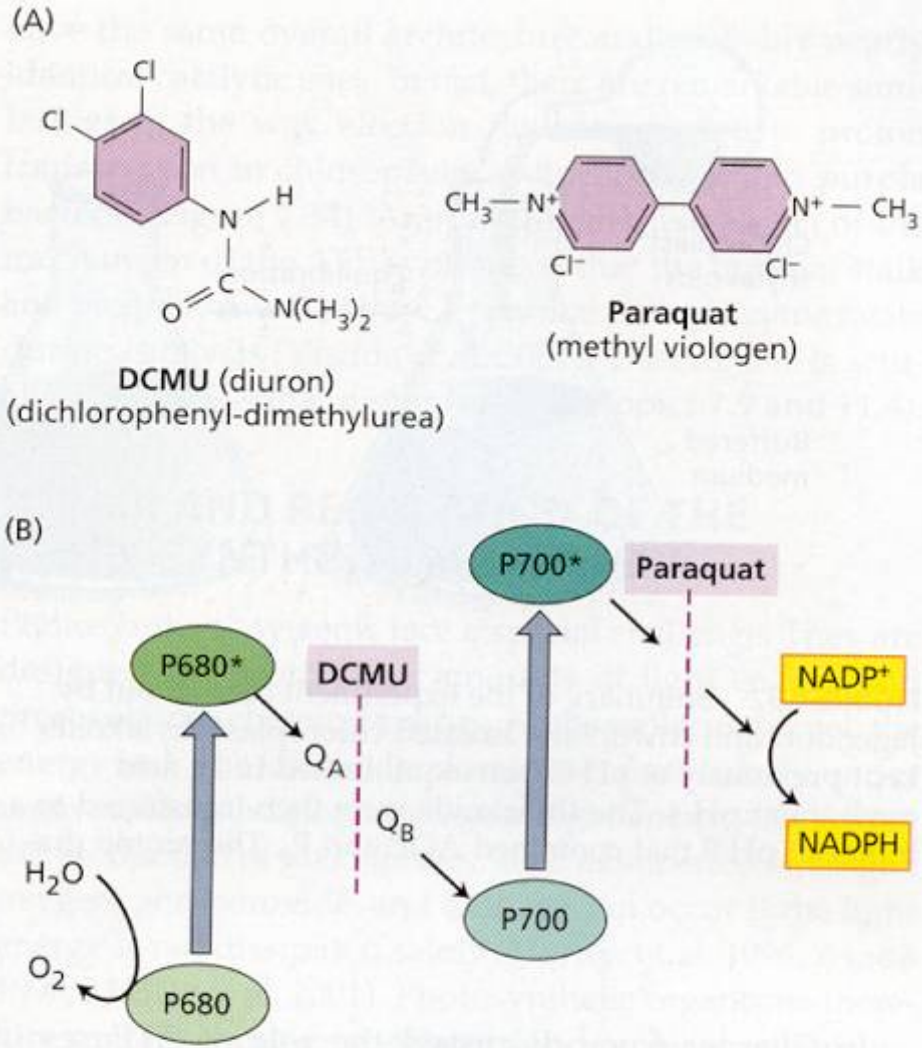

FIGURE 7.31 Chemical structure and mechanism of action of two important herbicides. (A) Chemical structure of dichlorophenyl-dimethylurea (DCMU) and methyl viologen (paraquat), two herbicides that block photosynthetic electron flow. DCMU is also known as diuron. (B) Sites of action of the two herbicides. DCMU blocks electron flow at the quinone acceptors of photosystem II, by competing for the binding site of plastoquinone. Paraquat acts by accepting electrons from the early acceptors of photosystem I.

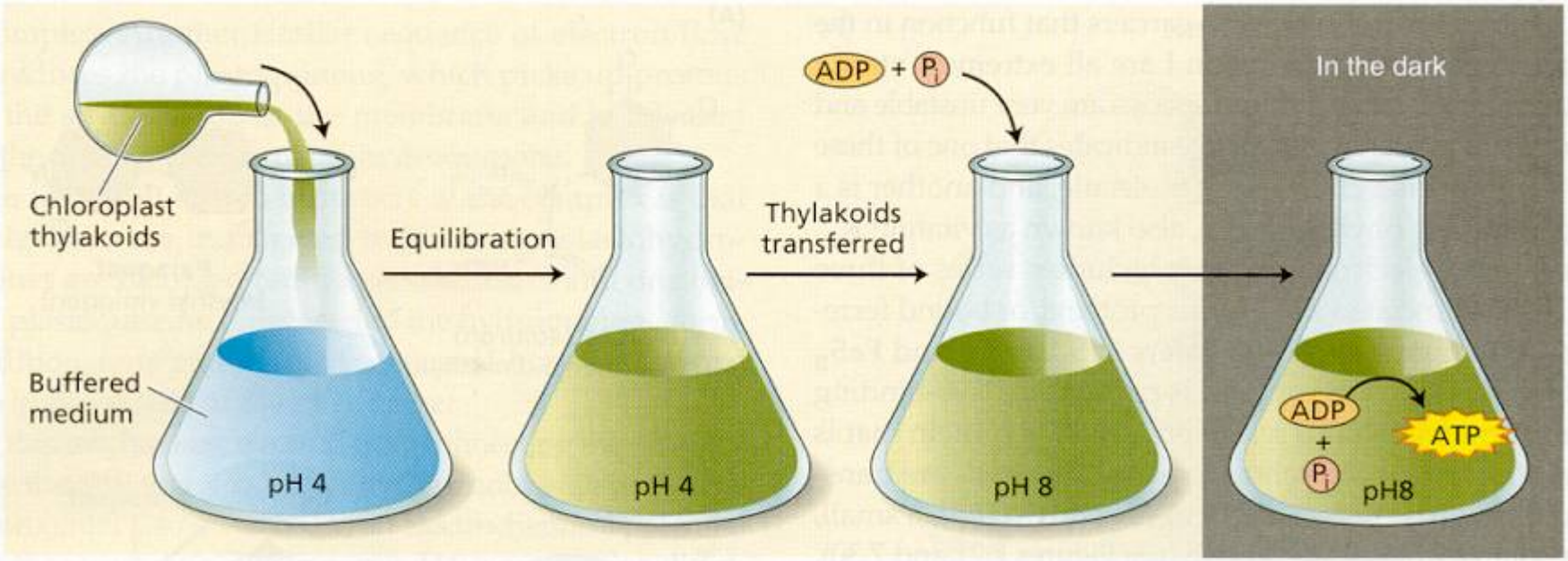

FIGURE 7.32 Summary of the experiment carried out by Jagendorf and coworkers. Isolated chloroplast thylakoids kept previously at pH 8 were equilibrated in an acid medium at pH 4. The thylakoids were then transferred to a buffer at pH 8 that contained ADP and P_i. The proton gradient generated by this manipulation provided a driving force for ATP synthesis in the absence of light. This experiment verified a prediction of the chemiosmotic theory stating that a chemical potential across a membrane can provide energy for ATP synthesis.

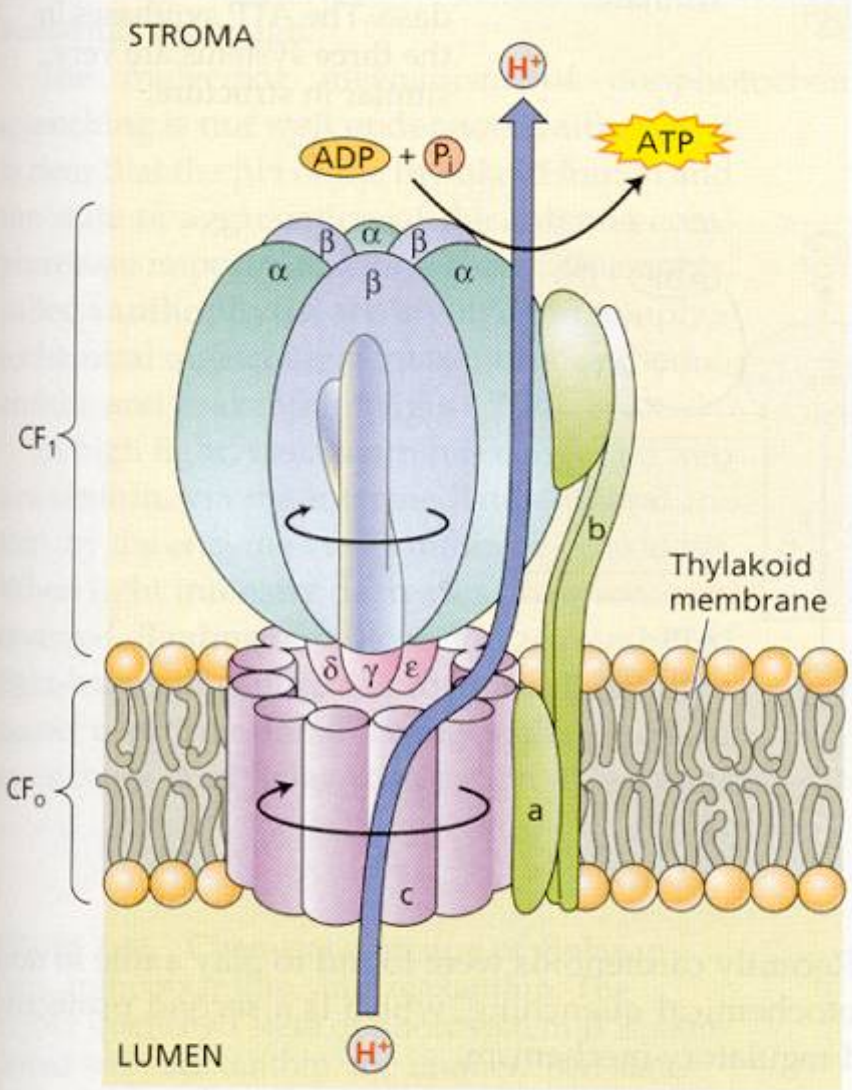

FIGURE 7.33 Structure of ATP synthase. This enzyme consists of a large multisubunit complex, CF_1, attached on the stromal side of the membrane to an integral membrane portion, known as CF_o. CF_1 consists of five different polypeptides, with a stoichiometry of α_3, β_3, γ, δ, ε. CF_o contains probably four different polypeptides, with a stoichiometry of a, b, b′, c_{12}.

(A) **Purple bacteria**

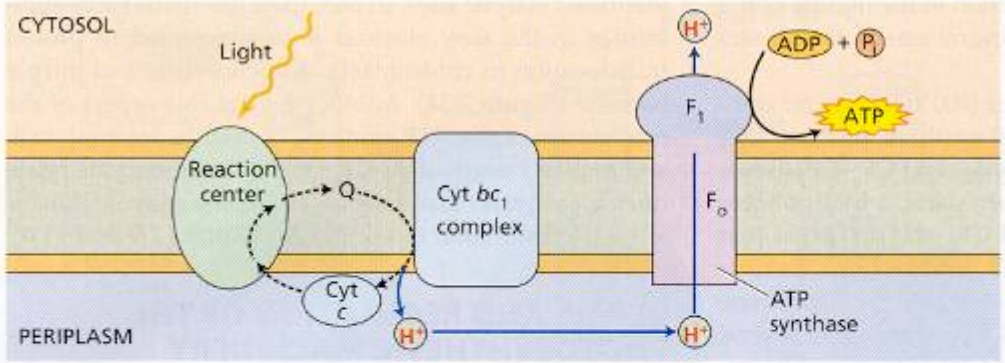

(B) **Chloroplasts**

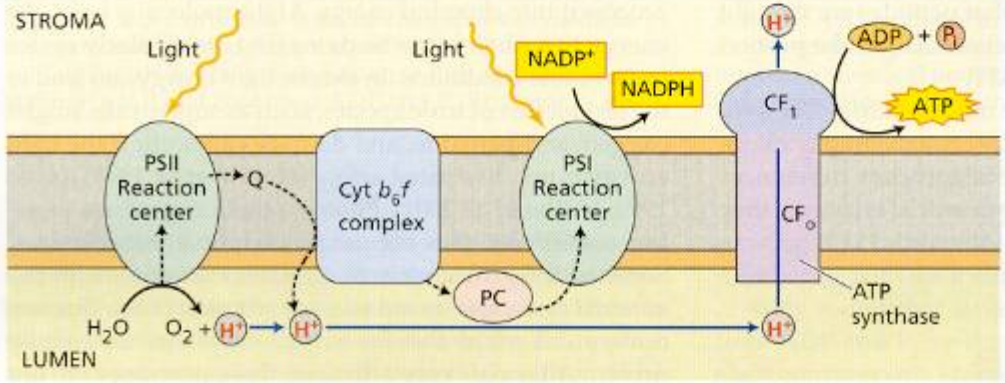

(C) **Mitochondria**

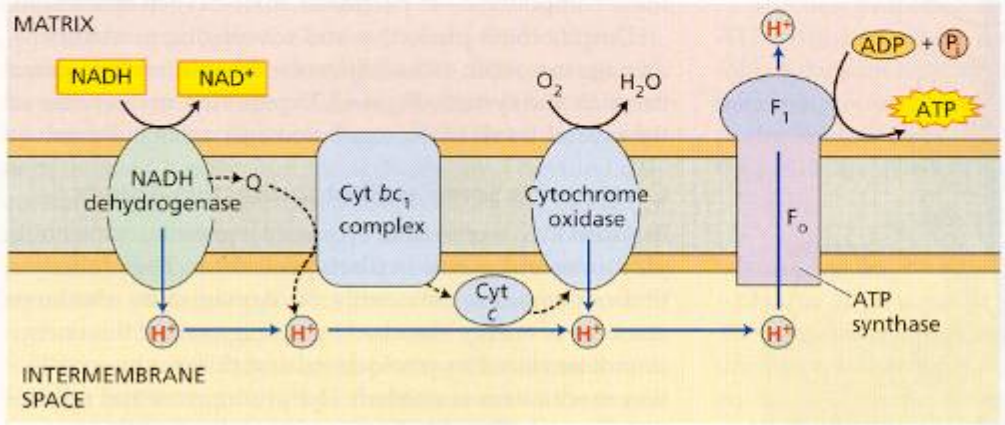

FIGURE 7.34 Similarities of photosynthetic and respiratory electron flow in bacteria, chloroplasts, and mitochondria. In all three, electron flow is coupled to proton translocation, creating a transmembrane proton motive force (Δp). The energy in the proton motive force is then used for the synthesis of ATP by ATP synthase. (A) A reaction center (RC) in purple photosynthetic bacteria carries out cyclic electron flow, generating a proton potential by the action of the cytochrome bc_1 complex. (B) Chloroplasts carry out noncyclic electron flow, oxidizing water and reducing $NADP^+$. Protons are produced by the oxidation of water and by the oxidation of PQH_2 (Q) by the cytochrome b_6f complex. (C) Mitochondria oxidize NADH to NAD^+ and reduce oxygen to water. Protons are pumped by the enzyme NADH dehydrogenase, the cytochrome bc_1 complex, and cytochrome oxidase. The ATP synthases in the three systems are very similar in structure.

FIGURE 7.35 Overall picture of the regulation of photon capture and the protection and repair of photodamage. Protection against photodamage is a multilevel process. The first line of defense is suppression of damage by quenching of excess excitation as heat. If this defense is not sufficient and toxic photoproducts form, a variety of scavenging systems eliminate the reactive photoproducts. If this second line of defense also fails, the photoproducts can damage the D1 protein of photosystem II. This damage leads to photoinhibition. The D1 protein is then excised from the PSII reaction center and degraded. A newly synthesized D1 is reinserted into the PSII reaction center to form a functional unit. (After Asada 1999.)

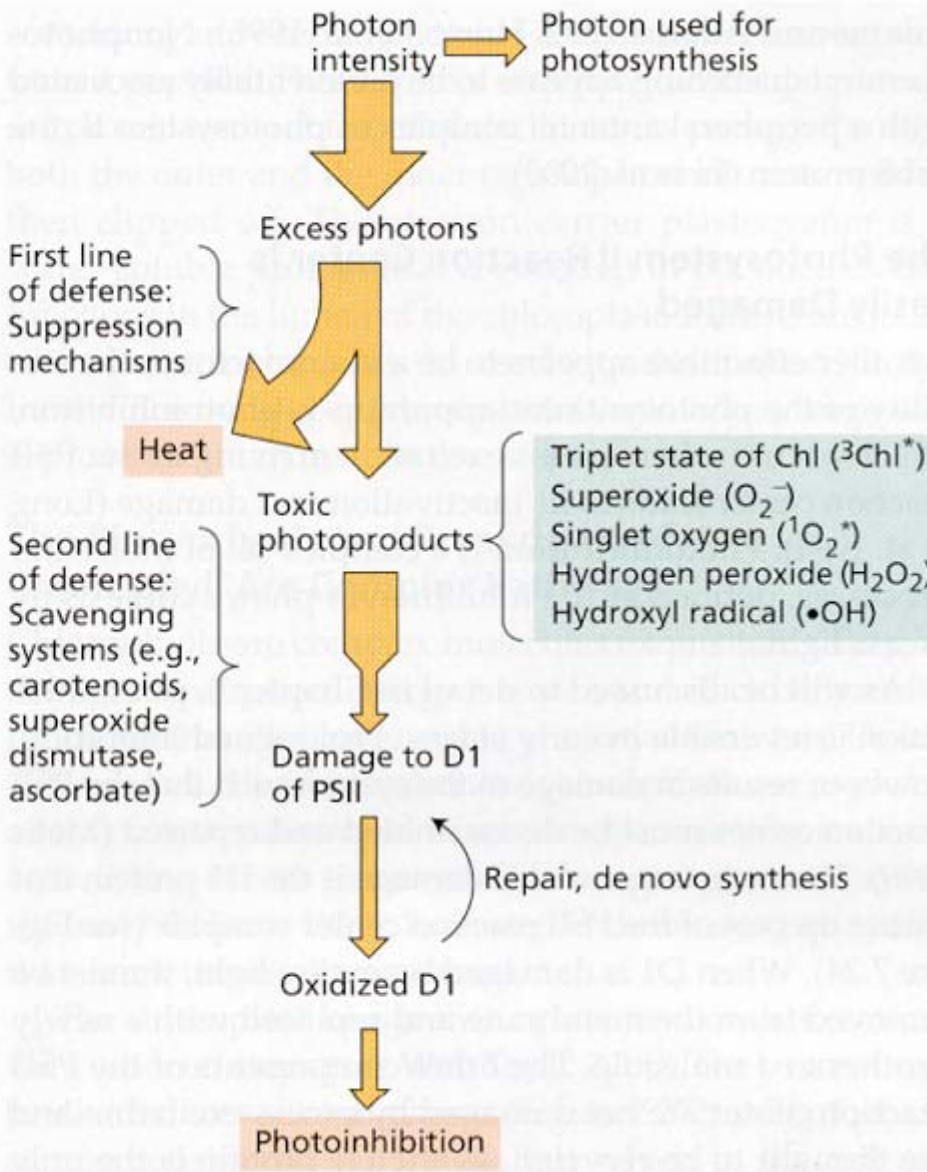

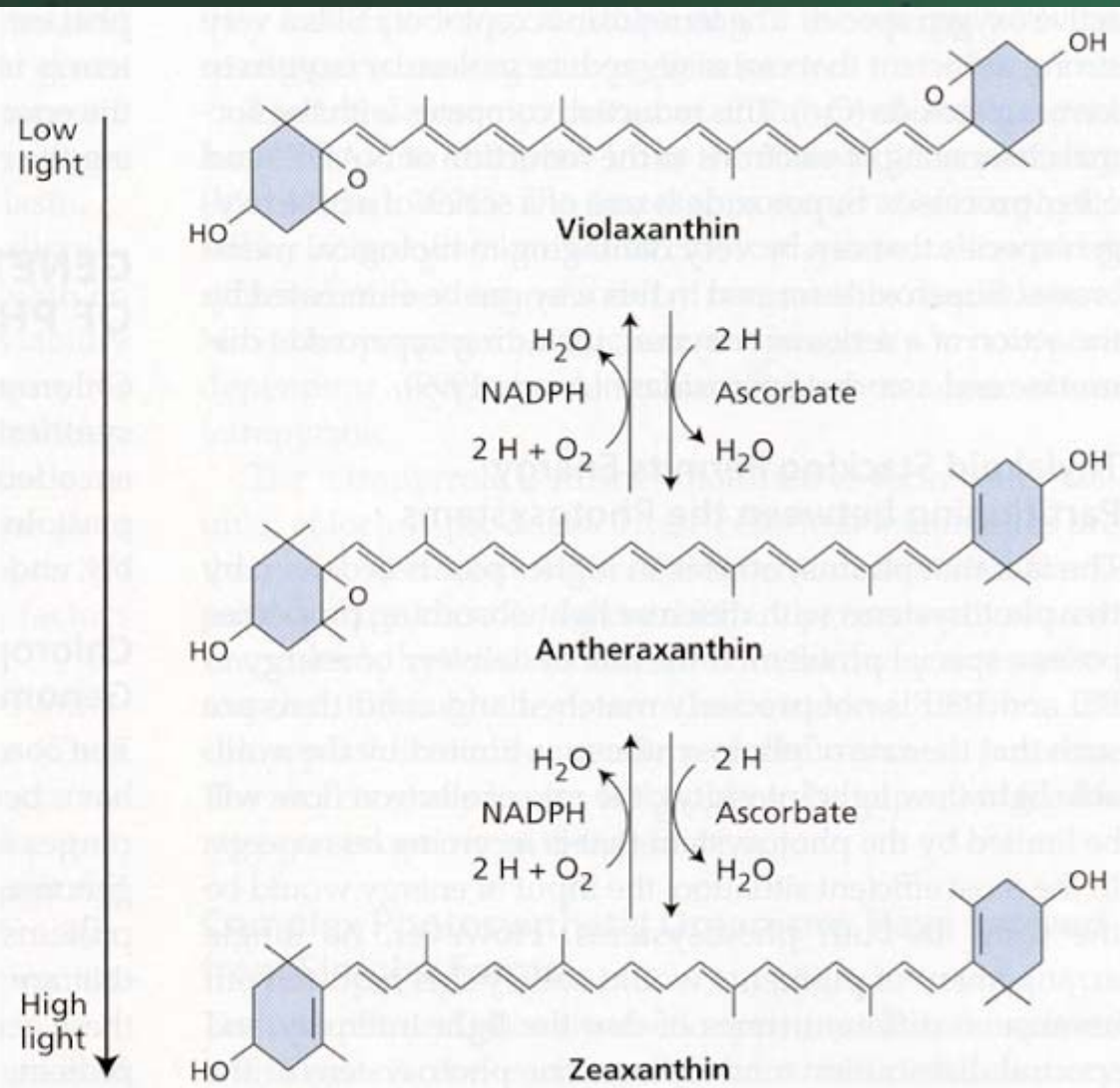

FIGURE 7.36 Chemical structure of violaxanthin, antheraxanthin, and zeaxanthin. The highly quenched state of photosystem II is associated with zeaxanthin, the unquenched state with violaxanthin. Enzymes interconvert these two carotenoids, with antheraxanthin as the intermediate, in response to changing conditions, especially changes in light intensity. Zeaxanthin formation uses ascorbate as a cofactor, and violaxanthin formation requires NADPH. (After Pfündel and Bilger 1994.)

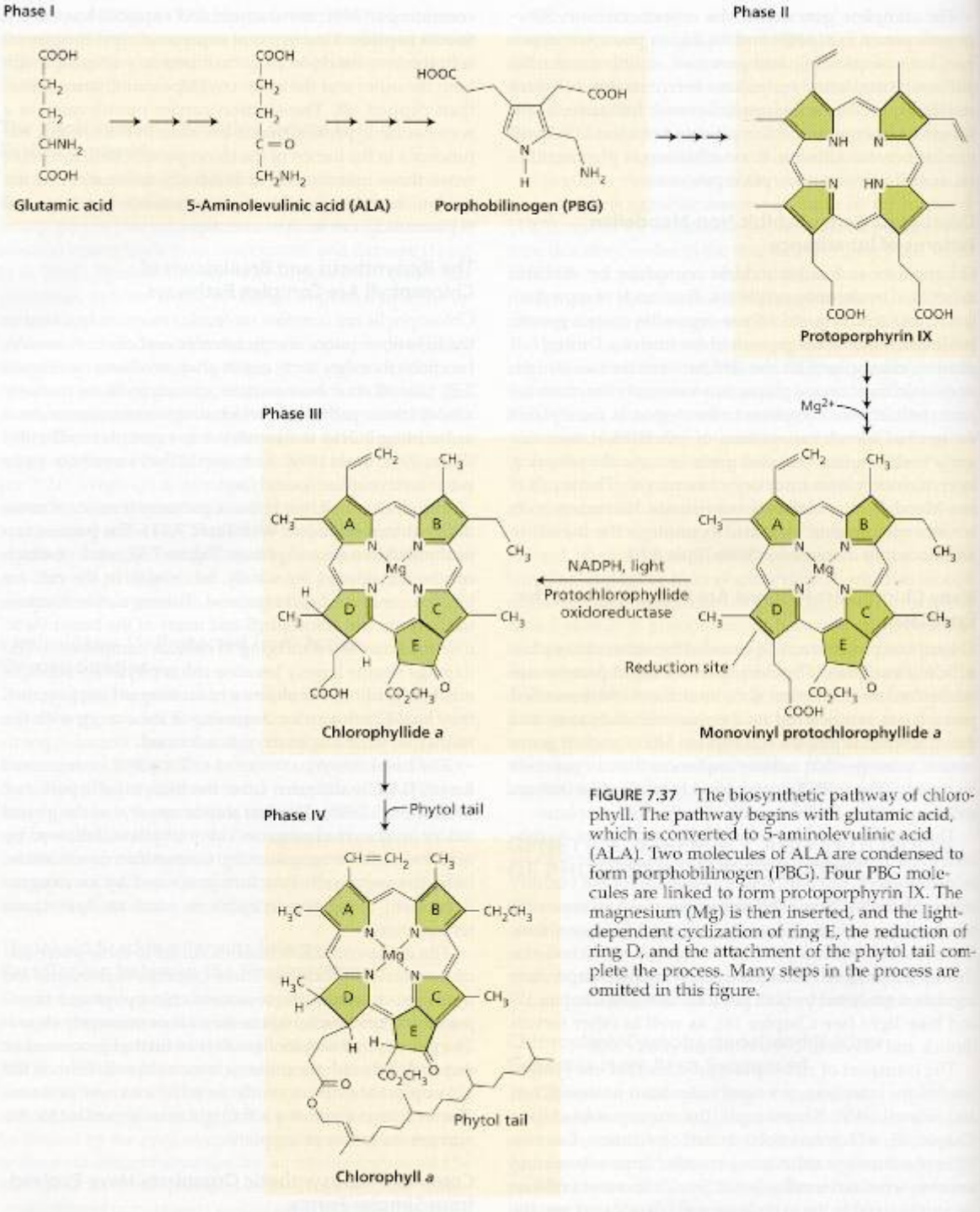

FIGURE 7.37 The biosynthetic pathway of chlorophyll. The pathway begins with glutamic acid, which is converted to 5-aminolevulinic acid (ALA). Two molecules of ALA are condensed to form porphobilinogen (PBG). Four PBG molecules are linked to form protoporphyrin IX. The magnesium (Mg) is then inserted, and the light-dependent cyclization of ring E, the reduction of ring D, and the attachment of the phytol tail complete the process. Many steps in the process are omitted in this figure.

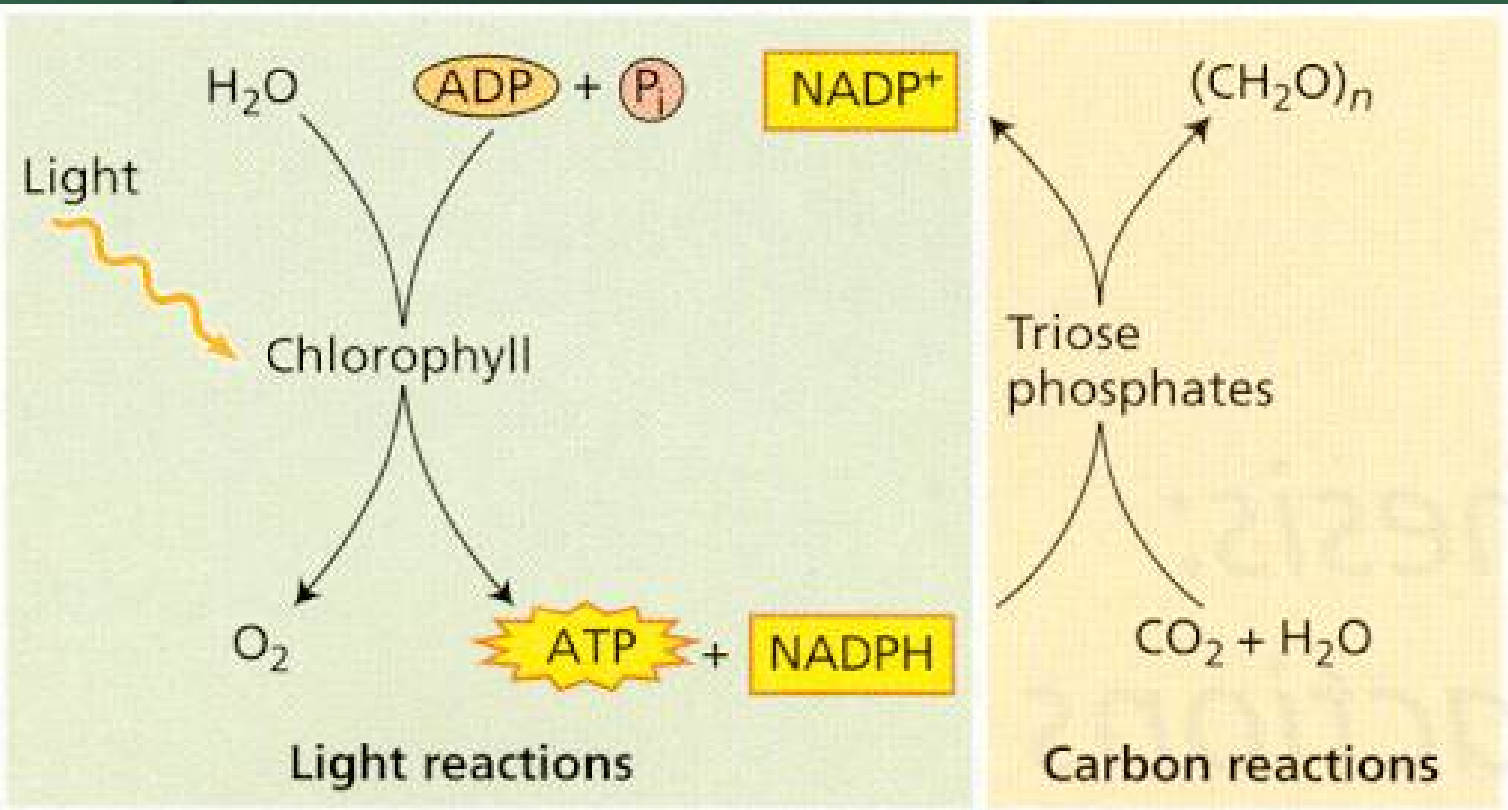

FIGURE 8.1 The light and carbon reactions of photosynthesis. Light is required for the generation of ATP and NADPH. The ATP and NADPH are consumed by the carbon reactions, which reduce CO_2 to carbohydrate (triose phosphates).

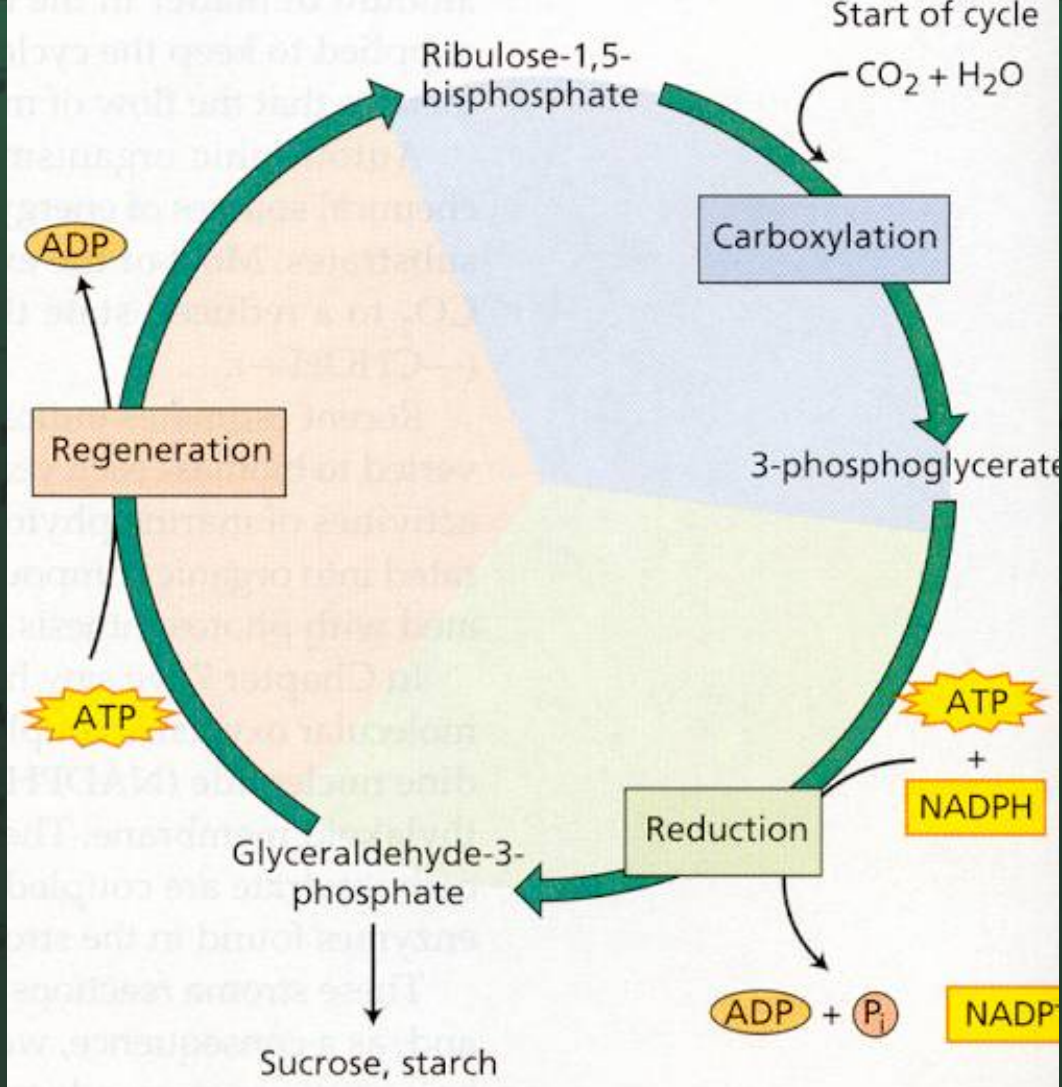

FIGURE 8.2 The Calvin cycle proceeds in three stages: (1) carboxylation, during which CO_2 is covalently linked to a carbon skeleton; (2) reduction, during which carbohydrate is formed at the expense of the photochemically derived ATP and reducing equivalents in the form of NADPH; and (3) regeneration, during which the CO_2 acceptor ribulose-1,5-bisphosphate re-forms.

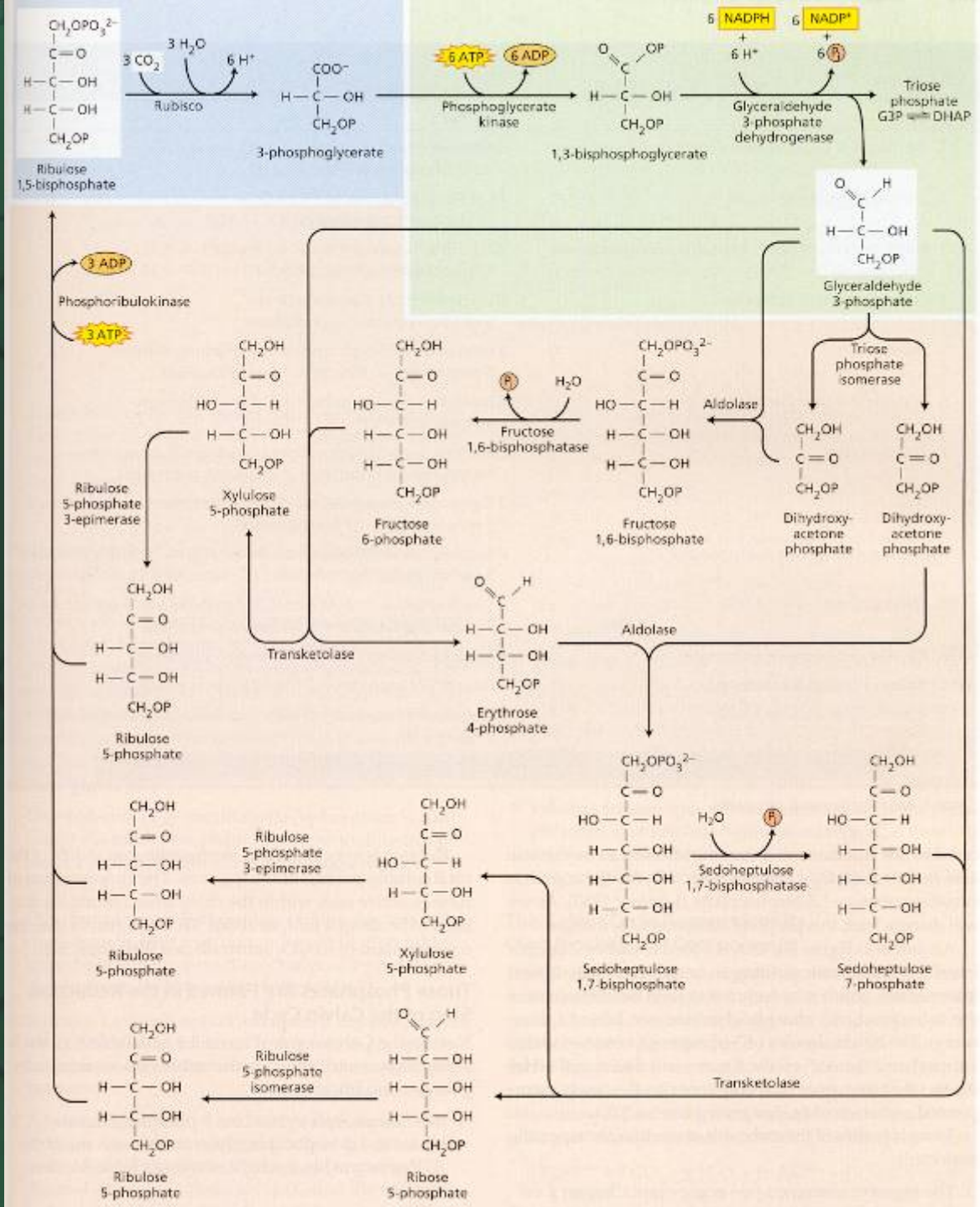
Ribulose 1,5-bisphosphate
3 CO2
3 H2O
6 H+
Rubisco
3-phosphoglycerate
6 ATP
6 ADP
Phosphoglycerate kinase
1,3-bisphosphoglycerate
6 NADPH
6 NADP+
6 H+
6 Pi
Glyceraldehyde 3-phosphate dehydrogenase
Triose phosphate G3P ⇌ DHAP
Glyceraldehyde 3-phosphate
3 ADP
Phosphoribulokinase
3 ATP
Triose phosphate isomerase
Aldolase
Fructose 1,6-bisphosphatase
Pi
H2O
Fructose 1,6-bisphosphate
Fructose 6-phosphate
Xylulose 5-phosphate
Dihydroxy-acetone phosphate
Dihydroxy-acetone phosphate
Ribulose 5-phosphate 3-epimerase
Transketolase
Aldolase
Erythrose 4-phosphate
Ribulose 5-phosphate
Ribulose 5-phosphate 3-epimerase
Xylulose 5-phosphate
Sedoheptulose 1,7-bisphosphatase
Sedoheptulose 1,7-bisphosphate
Sedoheptulose 7-phosphate
Ribulose 5-phosphate
Ribulose 5-phosphate isomerase
Transketolase
Ribulose 5-phosphate
Ribose 5-phosphate

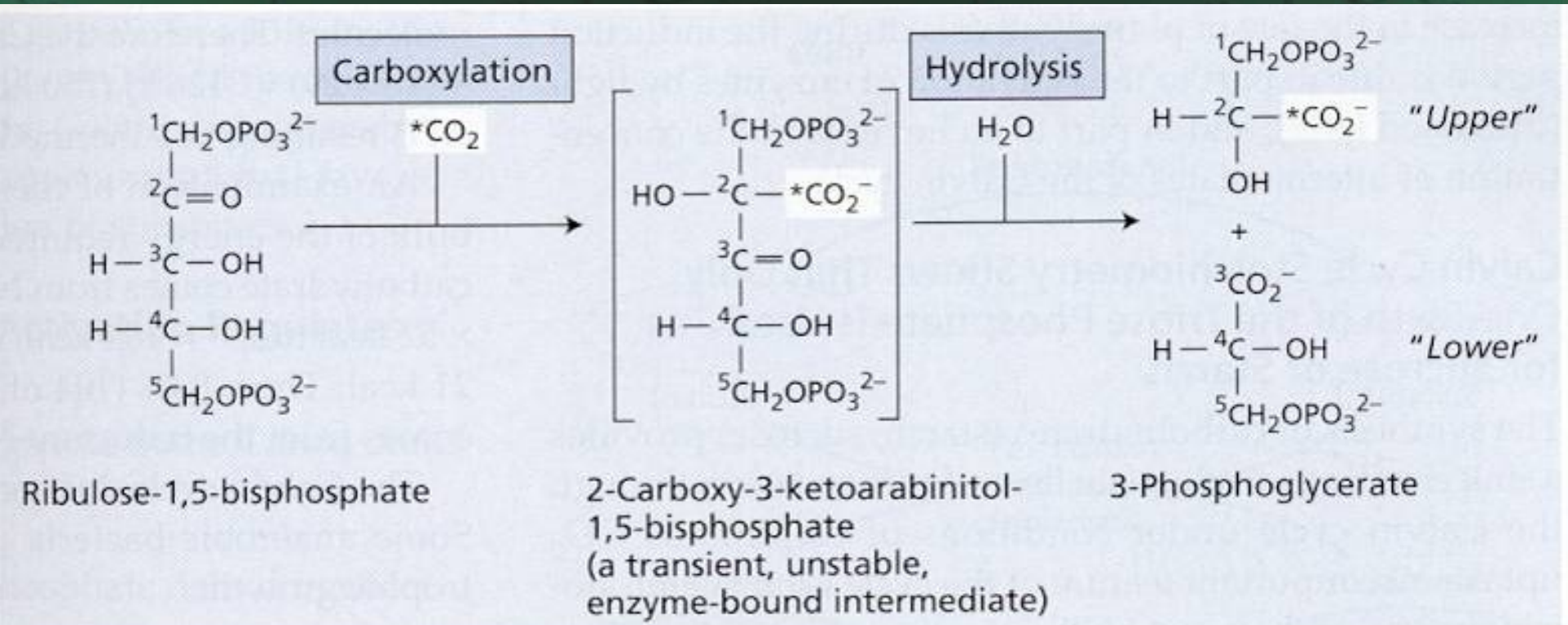

Ribulose-1,5-bisphosphate

2-Carboxy-3-ketoarabinitol-1,5-bisphosphate (a transient, unstable, enzyme-bound intermediate)

3-Phosphoglycerate

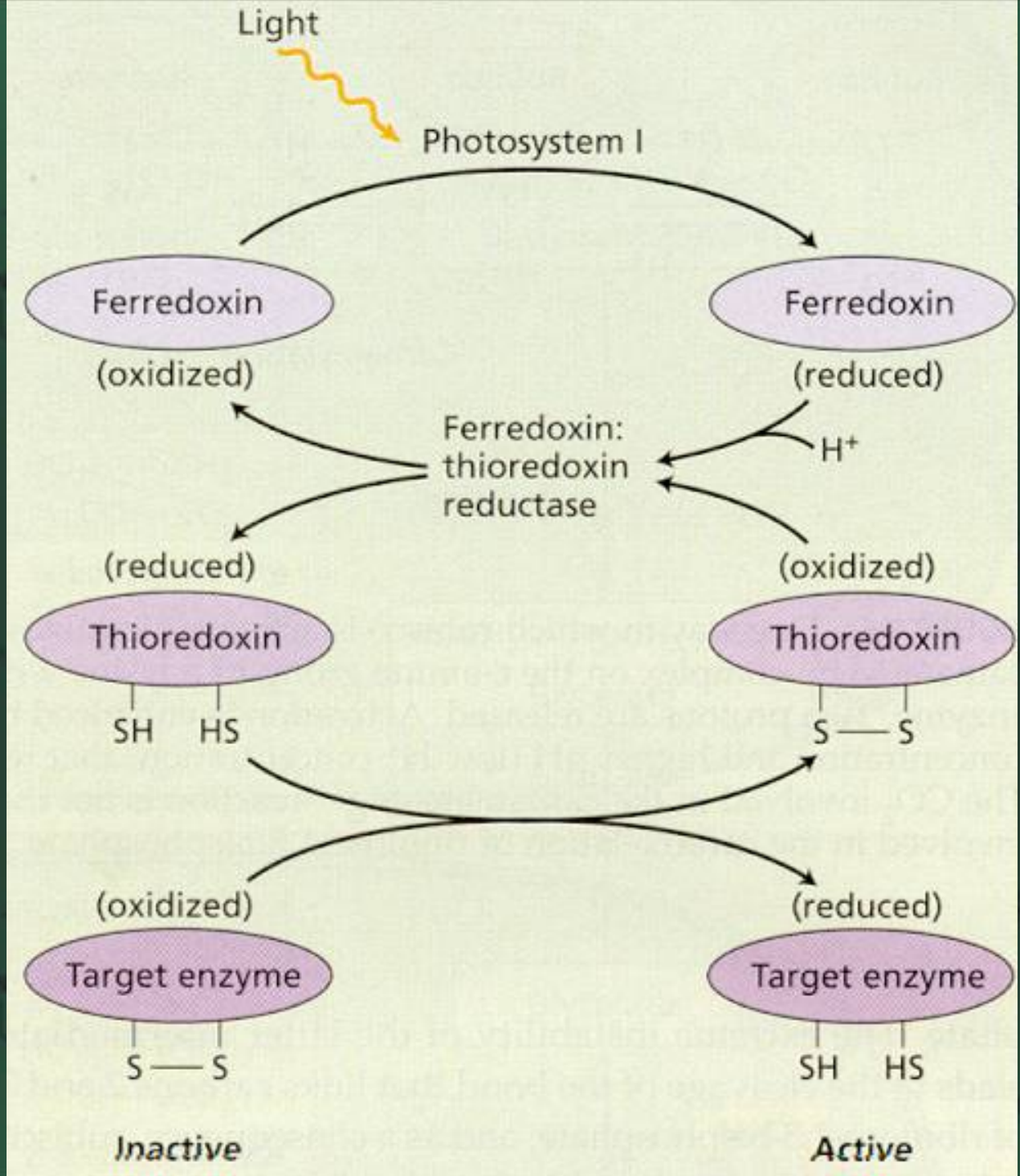
Light
Photosystem I
Ferredoxin
(oxidized)
Ferredoxin
(reduced)
Ferredoxin:
thioredoxin
reductase
H+
(reduced)
Thioredoxin
SH HS
(oxidized)
Thioredoxin
S — S
(oxidized)
Target enzyme
S — S
(reduced)
Target enzyme
SH HS
Inactive
Active

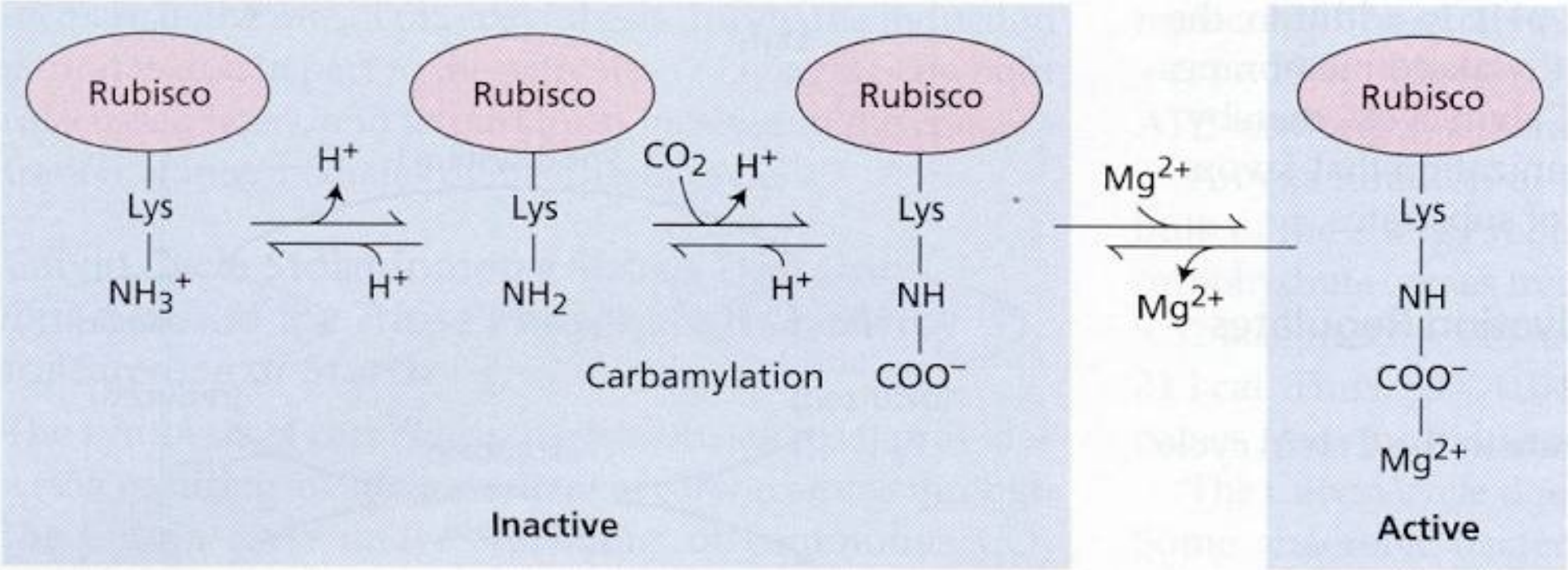

FIGURE 8.6 One way in which rubisco is activated involves the formation of a carbamate–Mg^{2+} complex on the ε-amino group of a lysine within the active site of the enzyme. Two protons are released. Activation is enhanced by the increase in Mg^{2+} concentration and higher pH (low H^+ concentration) that result from illumination. The CO_2 involved in the carbamate–Mg^{2+} reaction is not the same as the CO_2 involved in the carboxylation of ribulose-1,5-bisphosphate.

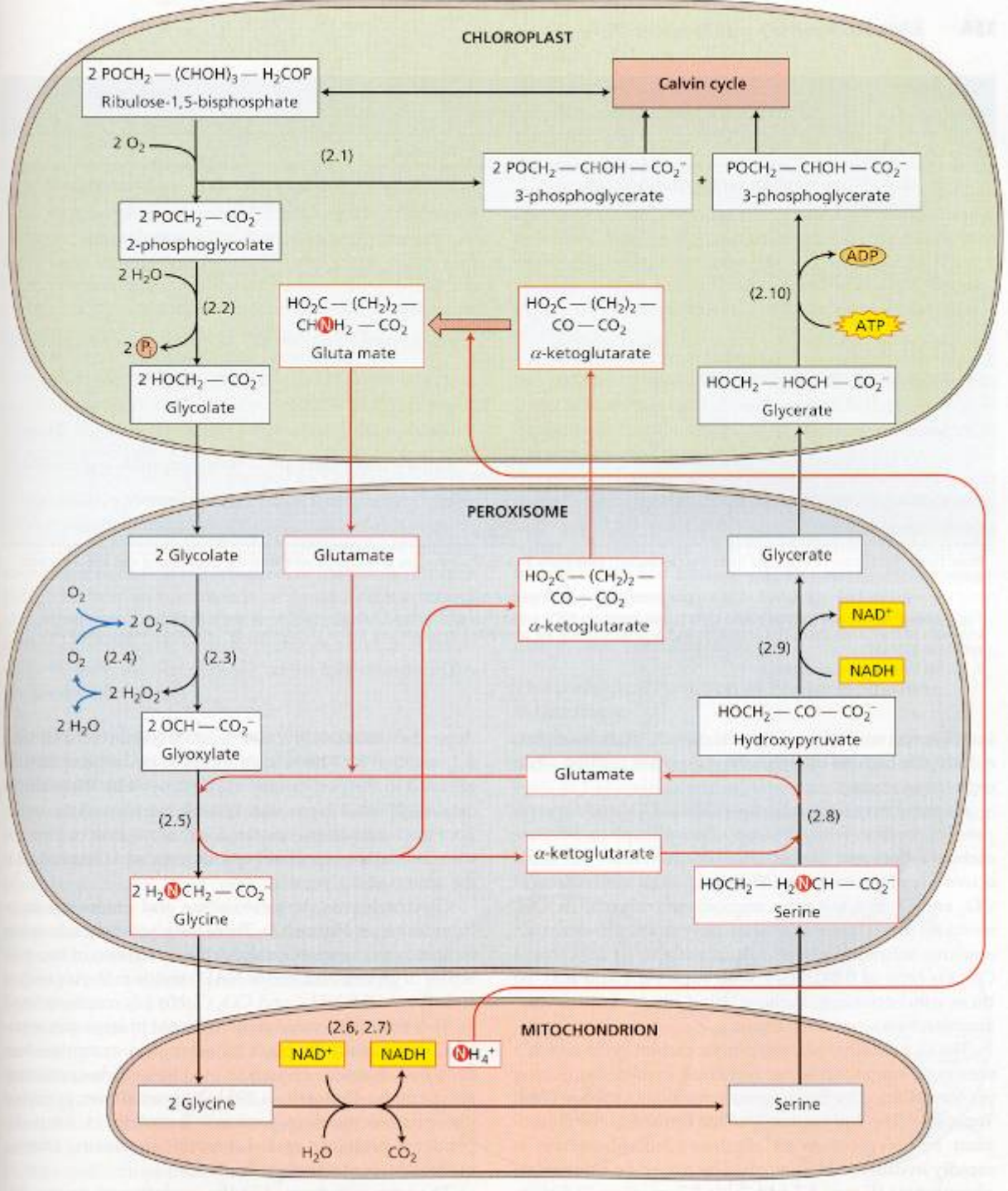
CHLOROPLAST
2 POCH2 — (CHOH)3 — H2COP
Ribulose-1,5-bisphosphate
Calvin cycle
2 O2
(2.1)
2 POCH2 — CHOH — CO2−
3-phosphoglycerate
POCH2 — CHOH — CO2−
3-phosphoglycerate
2 POCH2 — CO2−
2-phosphoglycolate
2 H2O
(2.2)
2 Pi
2 HOCH2 — CO2−
Glycolate
HO2C — (CH2)2 — CHNH2 — CO2
Gluta mate
HO2C — (CH2)2 — CO — CO2
α-ketoglutarate
(2.10)
ADP
ATP
HOCH2 — HOCH — CO2−
Glycerate
PEROXISOME
2 Glycolate
Glutamate
HO2C — (CH2)2 — CO — CO2
α-ketoglutarate
Glycerate
O2
2 O2
O2
(2.4)
(2.3)
2 H2O2
2 H2O
2 OCH — CO2−
Glyoxylate
(2.9)
NAD+
NADH
HOCH2 — CO — CO2−
Hydroxypyruvate
Glutamate
(2.5)
α-ketoglutarate
(2.8)
2 H2NCH2 — CO2−
Glycine
HOCH2 — H2NCH — CO2−
Serine
MITOCHONDRION
(2.6, 2.7)
NAD+
NADH
NH4+
2 Glycine
Serine
H2O
CO2